

OPEN ACCESS

Use of Multielectrode Arrays and Statistical Analysis to Investigate the Pitting Probability of Copper: Part II. The Effect of Sulfate and Bicarbonate

To cite this article: Sina Matin *et al* 2023 *J. Electrochem. Soc.* **170** 051503

View the [article online](#) for updates and enhancements.

You may also like

- [Spatial Interactions among Localized Corrosion Sites : Experiments and Modeling](#)
T. T. Lunt, J. R. Scully, V. Brusamarello et al.
- [Passivity and Pit Stability Behavior of Copper as a Function of Selected Water Chemistry Variables](#)
Hongbo Cong, Harold T. Michels and John R. Scully
- [Effect of Applied Potential on Pit Propagation in Copper as Function of Water Chemistry](#)
Hung Ha, Claes Taxén, Hongbo Cong et al.



Your Lab in a Box!

The PAT-Tester-i-16: All you need for Battery Material Testing.

- ✓ All-in-One Solution with integrated Temperature Chamber!
- ✓ Cableless Connection for Battery Test Cells!
- ✓ Fully featured Multichannel Potentiostat / Galvanostat / EIS!

www.el-cell.com +49 40 79012-734 sales@el-cell.com

EL-CELL[®]
electrochemical test equipment





Use of Multielectrode Arrays and Statistical Analysis to Investigate the Pitting Probability of Copper: Part II. The Effect of Sulfate and Bicarbonate

Sina Matin,¹ Adam Morgan,¹ Arezoo Tahmasebi,² Dmitriy Zadidulin,¹ Mehran Behazin,³ Matt Davison,² David W. Shoesmith,^{1,4} and James J. Noël^{1,4,*}

¹Department of Chemistry, Western University, London, ON, N6A 5B7, Canada

²Department of Statistical and Actuarial Sciences, Western University, London, ON, N6A 5B7, Canada

³Nuclear Waste Management Organization, Toronto, ON, M4T 2S3, Canada

⁴Surface Science Western, Western University, London, ON, N6G 0J3, Canada

Copper and copper alloys have found applications in various industries. One of the main reasons Cu and its alloys are utilized widely is that they have sufficient corrosion resistance in key environments, such as seawater and anoxic solutions; however, localized corrosion processes might occur in the presence of aggressive anions, oxygen, or an increase in solution pH. In critical applications of Cu, the susceptibility of Cu to localized corrosion, specifically pitting, must be carefully considered, as it could lead to material failure. In this study, the pitting probability of Cu in unary (sulfate) and binary (sulfate + bicarbonate) solutions was investigated using electrochemical techniques in conjunction with statistical analysis. We determined pitting probabilities based on two different defining criteria for pitting susceptibility, one based on the probability that the corrosion potential, E_{corr} , could exceed the passivity breakdown potential, E_b , and the other, a more conservative approach, based on the likelihood that E_{corr} would be greater than the repassivation potential, E_{rp} . The pitting probability of Cu did not change significantly with sulfate concentration at pH 8 but was found to increase with increasing $[\text{SO}_4^{2-}]$ up to 0.005 M at pH 9 and then to decrease with a further increase in $[\text{SO}_4^{2-}]$.

© 2023 The Author(s). Published on behalf of The Electrochemical Society by IOP Publishing Limited. This is an open access article distributed under the terms of the Creative Commons Attribution 4.0 License (CC BY, <http://creativecommons.org/licenses/by/4.0/>), which permits unrestricted reuse of the work in any medium, provided the original work is properly cited. [DOI: 10.1149/1945-7111/acd606]



Manuscript submitted November 6, 2022; revised manuscript received May 12, 2023. Published May 25, 2023. *This paper is part of the JES Focus Issue on Critical Factors in Localized Corrosion in Honor of Gerald Frankel.*

Supplementary material for this article is available [online](#)

Many industries have been using Cu and its alloys as the primary materials in their products and equipment (e.g., water pipes, heat exchangers, etc.), due to their mechanical and physical properties. From both longevity and economic points of view, Cu has attracted the attention of the nuclear industry as a candidate for the corrosion barrier for used fuel containers (UFC) in a deep geological repository (DGR). Based on the current design, the UFCs will be coated (Canada) or covered (Sweden) with high-purity Cu as a corrosion barrier.^{1–12}

Cu oxide films are commonly present on Cu depending on the application. For example, formation of scale and Cu oxides in heat exchangers results in a decrease in heat transport efficiency. However, in corrosive environments, oxide films can protect Cu from further dissolution. In specific situations, Cu is not able to form a dense and sufficiently protective oxide film on the surface, which can lead to material failure by corrosion.^{13–22}

Cu is thermodynamically stable in most oxygen-free environments. However, under aerated conditions, corrosion, specifically localized corrosion in the form of pitting, becomes a possibility. The morphology and protectiveness of a passive oxide film depends on both material properties, such as the grain size and orientation, and environmental conditions, such as the concentration of aggressive anions, exposure time, etc.^{23–36} Protective films can be formed on the surface of Cu by either the dissolution-precipitation mechanism or a solid-state reaction involving nucleation and growth, with the latter leading to a passive film.^{35–38} In moderately alkaline solutions, Cu forms a dual-layer film comprised of an inner Cu_2O layer and an outer CuO or/and $\text{Cu}(\text{OH})_2$ layer.^{31,35,39–41} During the initial film growth, due to the porous structure of the Cu_2O layer, dissolution as Cu^{2+} cations can occur at the Cu surface, provided that the potential is sufficiently positive, with the Cu^{2+} cations diffusing from the Cu surface to the oxide-solution interface, leading to the deposition of

CuO and/or $\text{Cu}(\text{OH})_2$ on top of the Cu_2O inner layer,^{29,35,42–44} and in some cases, passivation.

Passive film breakdown mechanisms have been extensively investigated, and two main mechanisms proposed. The first mechanism involves the transport of aggressive anions from the solution into the oxide film, leading eventually to the generation of stress within the film which causes its mechanical breakdown.⁴⁵ The second mechanism involves the adsorption of aggressive anions on the passive film resulting in its thinning and the eventual exposure of the metal surface.^{46,47}

The susceptibility of materials to pitting corrosion can be determined by a comparison of the corrosion potential (E_{corr}) to the passive film breakdown potential (E_b) measured by a potentiodynamic scan of the applied potential (E) from low to high values, or, more conservatively, by a comparison of E_{corr} to the repassivation potential (E_{rp}) measured by a potentiodynamic scan of E from high to lower values on an electrode already undergoing pitting corrosion. All corrosion parameters such as E_{corr} , E_b , and E_{rp} (the potential at which the current on the negative-going scan matches the original passive current observed on the positive-going scan) are distributed values, due to uncontrollable variations in oxide film properties and reactivity, variations in the local environment at the oxide surface, as well as the stochastic nature of passive film rupture.^{39,48} According to one definition, pitting is deemed to be possible if $E_{\text{corr}} \geq E_b$,^{31,39,49} with the distribution of values making the boundary between immunity from and susceptibility to pitting uncertain. A statistical approach to determining the probability that pitting could occur under a given set of conditions is necessary, since both E_{corr} and E_b can assume a range of values (i.e., neither is single-valued). A more conservative assessment of pitting probability involves evaluating the difference between E_{corr} and E_{rp} values. The E_{rp} can be determined by scanning E in the negative direction from a value above E_b , on an electrode that is already undergoing pitting corrosion, until the measured current drops to the value previously measured in the passive region on an identical electrode exposed to the same environment. The values of E_{rp} depend on a variety of

*Electrochemical Society Fellow.

^zE-mail: jjnoel@uwo.ca

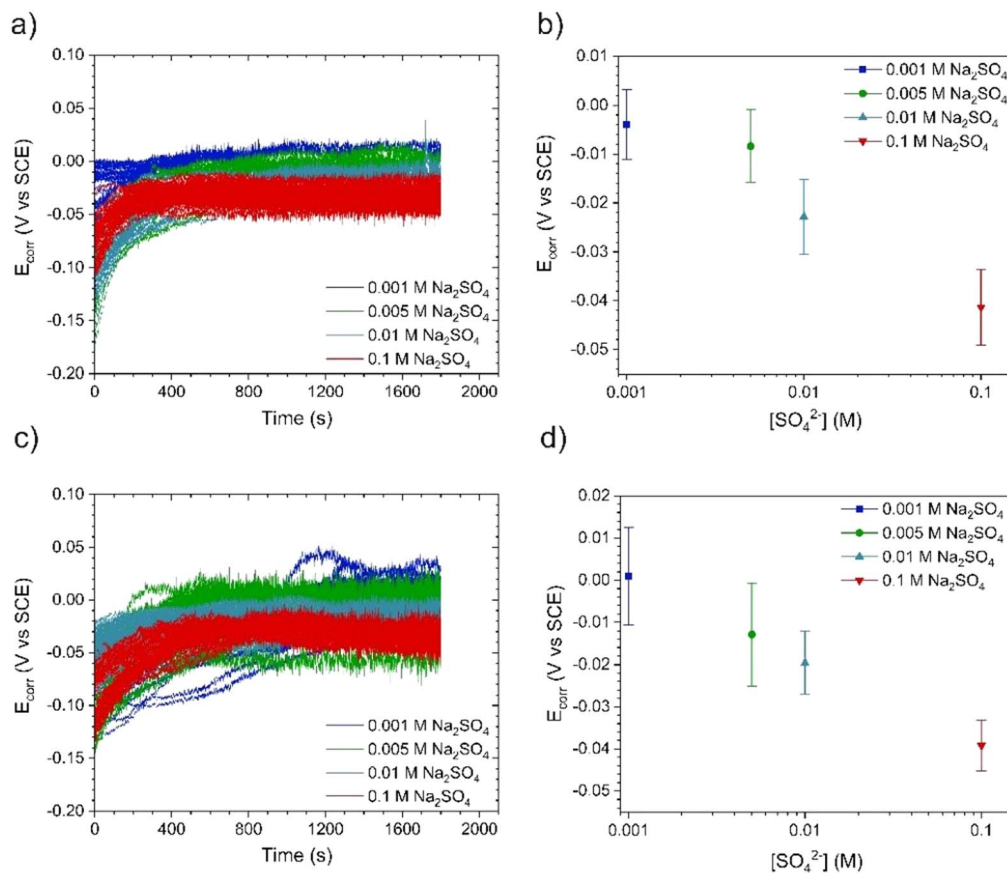


Figure 1. Corrosion potential of Cu electrodes; (a) E_{corr} of Cu in a solution containing 0.001, 0.005, 0.01, and 1 M SO_4^{2-} at pH 8, (b) Comparison of mean and standard deviation of Cu electrodes in a solution containing 0.001, 0.005, 0.01, and 1 M SO_4^{2-} at pH 8, (c) E_{corr} of Cu in a solution containing 0.001, 0.005, 0.01, and 1 M SO_4^{2-} at pH 9, and (d) Comparison of mean and standard deviation of Cu electrodes in a solution containing 0.001, 0.005, 0.01, and 1 M SO_4^{2-} at pH 9.

factors, such as pit depth, maximum dissolution current density ($i_{\text{diss,max}}$), the potential scan rate used in potentiodynamic polarization measurements such as those described in this study, and the pit initiation rate.⁵⁰ The E_{rp} is inversely proportional to the pit depth and $i_{\text{diss,max}}$, so increasing the pit depth and $i_{\text{diss,max}}$ both result in lower E_{rp} . However, E_{rp} is directly proportional to the scan rate and the pit initiation rate, since lower scan rates and/or pit initiation rates provide more time for pits to grow deeper, thus leading to a lower E_{rp} .

Many studies have been conducted to elucidate the influence of various parameters, such as anion concentrations, pH, and temperature, on E_{corr} , E_b , and E_{rp} .^{39,48,51–60} The previous research found that CO_3^{2-} and OH^- enhance the passive film stability, while Cl^- and SO_4^{2-} have an aggressive effect on Cu and stainless steel.^{51,53,56,58–62} The dependence of passive film stability of Cu on $[\text{Cl}^-]$ has been examined extensively. The results indicate that the corrosion rate increases with increasing $[\text{Cl}^-]$ up to a certain concentration ($[\text{Cl}^-]_{\text{crit}}$), above which chloride plays an inhibiting role, due to the rapid formation of a CuCl layer.^{59,60,63,64} The pitting probability of Cu can also be influenced by the pH of the solution.^{60,65} Cong³⁹ proposed three different regions based on pH: uniform corrosion for $\text{pH} < 7$; a pitting susceptibility region between $\text{pH} 7$ and 10; and limited susceptibility for $\text{pH} > 10$. It is important to note that the boundary between these regions depends on temperature, $[\text{O}_2]$, and solution composition. E_{corr} , E_b , and E_{rp} were found to depend on the concentrations of different anions (Cl^- , SO_4^{2-} , $\text{HCO}_3^-/\text{CO}_3^{2-}$, OH^-). Generally, Cl^- and SO_4^{2-} destabilized the passive films, leading to decreases in E_{corr} and E_b . However, the effect of SO_4^{2-} is still ambiguous and requires more research effort. The presence of $\text{HCO}_3^-/\text{CO}_3^{2-}$ enhanced the

durability of the passive film resulting in higher E_{corr} and E_b values. The properties of the passive film are particularly important when materials are in contact with solutions containing low concentrations of aggressive anions, resulting in film breakdown at relatively high potentials.^{66,67} The substitution of O^{2-} ions with aggressive anions such as Cl^- and SO_4^{2-} in an oxide film leads to the creation of defects which render the film less protective.^{9,10,63,68}

The corrosion behaviour of Cu in different environments, such as seawater and deaerated solutions, is well established. In addition, Matin et al.⁶⁹ investigated the pitting probability of Cu in chloride-containing solutions using multielectrode arrays and statistical analysis, but there is a lack of information regarding the susceptibility of Cu to pitting corrosion in sulfate-containing solutions. The majority of the published research has been conducted based on the hypothesis that corrosion parameters are deterministic, thus ignoring the effect of distributed values. Qin et al.⁵² defined the approximate active/passive boundary as a function of $[\text{SO}_4^{2-}]$ and pH. This boundary was developed based on only a small number of experiments and does not account for the statistical distributions of the parameters measured to establish it. A more thorough understanding of the pitting probability of Cu in SO_4^{2-} and HCO_3^- solutions requires the application of a method that accounts for the distributed nature of the corrosion parameters. In the studies described in this research, a Cu multielectrode array was used to determine the distributions of E_{corr} , E_b , and E_{rp} by simultaneously monitoring 30 electrodes simultaneously exposed to the same solution. Each experiment was performed twice, with 60 data points collected in total for each corrosion parameter, including E_{corr} , E_b , and E_{rp} . The in-depth process and methodology can be found in our previous paper.⁶⁹

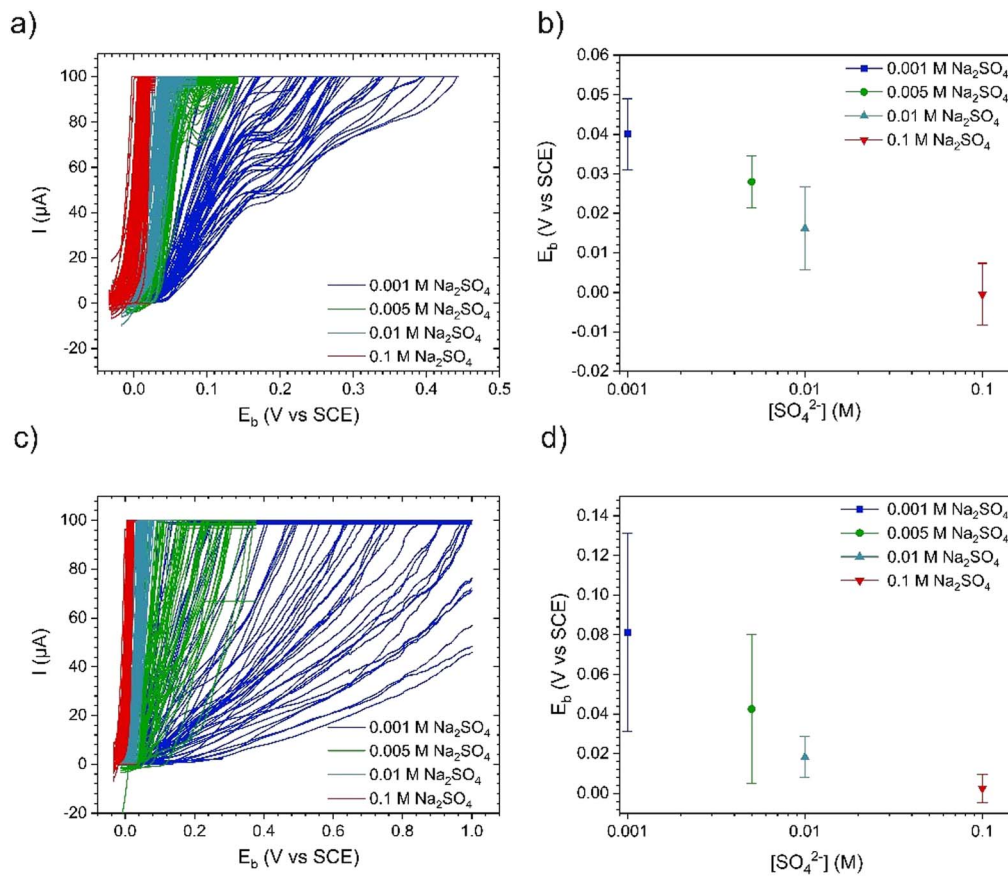


Figure 2. Breakdown potential of Cu electrodes (a) E_b of Cu in a solution containing 0.001, 0.005, 0.01, and 1 M SO_4^{2-} at pH 8 (b) Comparison of mean and standard deviation of Cu electrodes in a solution containing 0.001, 0.005, 0.01, and 1 M SO_4^{2-} at pH 8 (c) E_b of Cu in a solution containing 0.001, 0.005, 0.01, and 1 M SO_4^{2-} at pH 9 (d) Comparison of mean and standard deviation of Cu electrodes in a solution containing 0.001, 0.005, 0.01, and 1 M SO_4^{2-} at pH 9.

Experimental Methodology

Sample preparation.—O-free and P-doped wrought Cu was supplied by the Swedish Nuclear Fuel and Waste Management Company (SKB, Stockholm, Sweden). Electrodes were machined in the form of bullet samples rounded at the edges to avoid edge effects during electrochemical experiments. A threaded connection to a stainless steel rod enabled connection to external electrochemical equipment. Figure of electrodes can be found here.⁶⁹ Specimens used in corrosion experiments were ground with a sequence of SiC papers with grit sizes of 600, 800, 1200, 2500, and 4000 followed by rinsing in type I water. The samples were then sonicated in ethanol to remove grinding residues and organic contaminants, and finally dried in a stream of Ar gas.

Solution Preparation

Solutions were prepared with reagent-grade sodium sulfate (Na_2SO_4 , 99.0%) and sodium bicarbonate (NaHCO_3 , 99.5%), provided by Fisher Scientific, and Type I water with a resistivity of 18.2 M Ω cm, prepared using a Thermo Scientific Barnstead Nanopure 7143 system. The multielectrode array, explained in our previous paper,⁶⁹ was exposed to either sulfate-containing solutions with various $[\text{SO}_4^{2-}]$ in the range from 0.001 M to 0.1 M or binary solutions containing 0.01 M SO_4^{2-} and various $[\text{HCO}_3^-]$. The pH of the solutions was adjusted to 8 and 9 by adding small volumes of NaOH.

Electrochemical Cell, Instrumentation, and Procedure

All electrochemical experiments were performed in a conventional three-electrode electrochemical cell using the multielectrode

array, a Pt plate as the counter electrode, and a saturated calomel reference electrode (SCE, 0.242 V vs SHE). The counter electrode had a large surface area (200 cm²) and was not a limiting factor in the current measurements. The electrochemical cell was placed inside a Faraday cage to reduce electrical noise from external sources. Following E_{corr} measurements, potentiodynamic polarization experiments were conducted at 10 mV min⁻¹ using a Multichannel Microelectrode Analyzer 910 (MMA, Scribner Associates) connected to a computer equipped with MMAlive software. The instrument was equipped with 100 μA zero resistance ammeters (ZRA). A schematic illustration of the experimental arrangement and photographs of the setup and array configuration can be found in our previous paper.⁶⁹ The E_b and E_{tp} values were measured in separate experiments to ensure that, when measuring E_{tp} , all 30 Cu specimens had experienced passive film breakdown.

Breakdown Potential (E_b) Measurements

Values of E_b were measured in a potentiodynamic scan. Prior to the scan, Cu electrodes were cathodically cleaned at -0.85 V vs SCE for 3 min, a procedure known to help improve the reproducibility of many electrochemical experiments.⁶⁹ Then, the corrosion potential (E_{corr}) was monitored for 30 min to allow a steady state to be established and to determine the range of values for the 30 electrodes on the multielectrode array. The potential was then scanned from E_{corr} in the positive direction at a scan rate of 10 mV min⁻¹ until the current on all electrodes reached 100 μA . The E_b was determined from the intersection of the tangent to the current in the passive range and the tangent to the rising current in the potential range after breakdown.^{63,70} A schematic of this procedure can be accessed through our previous paper.⁶⁹ Two runs using 30 electrodes each were conducted for each set of experimental conditions.

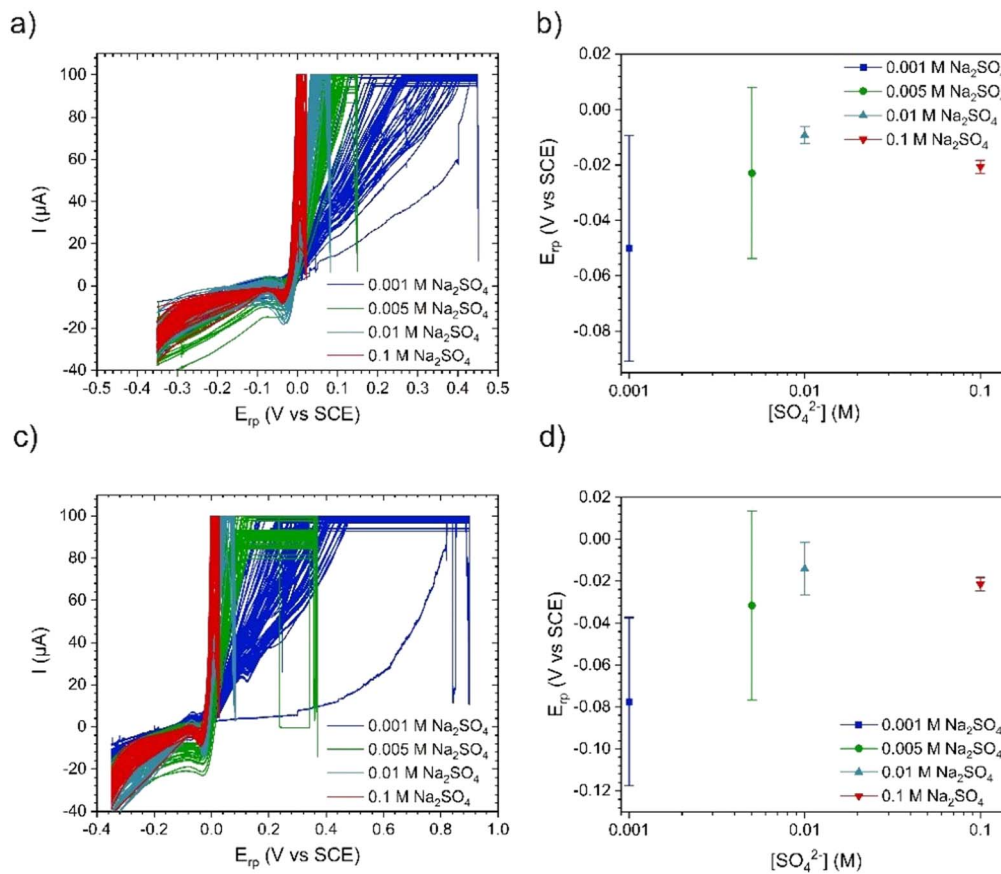


Figure 3. Repassivation potential of Cu electrodes (a) E_{rp} of Cu in a solution containing 0.001, 0.005, 0.01, and 1 M SO_4^{2-} at pH 8 (b) Comparison of mean and standard deviation of Cu electrodes in a solution containing 0.001, 0.005, 0.01, and 1 M SO_4^{2-} at pH 8 (c) E_{rp} of Cu in a solution containing 0.001, 0.005, 0.01, and 1 M SO_4^{2-} at pH 9 (d) Comparison of mean and standard deviation of Cu electrodes in a solution containing 0.001, 0.005, 0.01, and 1 M SO_4^{2-} at pH 9.

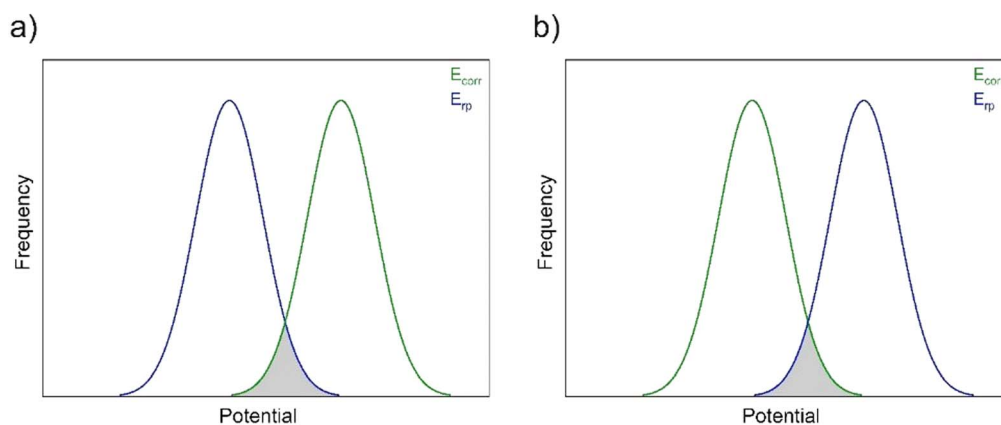


Figure 4. Overlap between distributions of corrosion potential and repassivation potential. Probability can be measured from the overlap of distribution functions when the distribution of corrosion potentials is located to the right of the distribution of repassivation potentials. (b) the pitting probability is the overlap between the distributions of E_{corr} and E_{rp} , when the distribution curve of E_{corr} is located on the left side of the distribution curve of E_{rp} (when the distribution curve of E_{corr} is located on the right side of the distribution curve of E_{rp} or the overlap is complete, then the pitting probability is 100%).

Repassivation Potential (E_{rp}) Measurements

To achieve a starting condition that was as nearly identical as possible for all electrodes in each experiment, the Cu surfaces were prepared as described in Section Sample preparation, then cathodic cleaning and E_{corr} measurement were performed. Next, a potential equal to the highest breakdown potential previously determined in E_b scans under the same conditions was applied to stimulate passive film breakdown on every electrode in the array. The potential was then scanned in the negative direction at a rate of 10 mV min^{-1} until

the current on each electrode reached the mean passive current previously determined in E_b scans under the same conditions. Please check Figs. 3, 4b, and 4d in our previous article to view the schematic of the procedure and learn more about how to determine E_b and E_{rp} .⁶⁹

The potential at which this current was achieved on each electrode was taken as the E_{rp} value for that electrode. Two runs using 30 electrodes each were conducted for each set of experimental conditions. We note that we conducted these experiments in naturally aerated solutions.

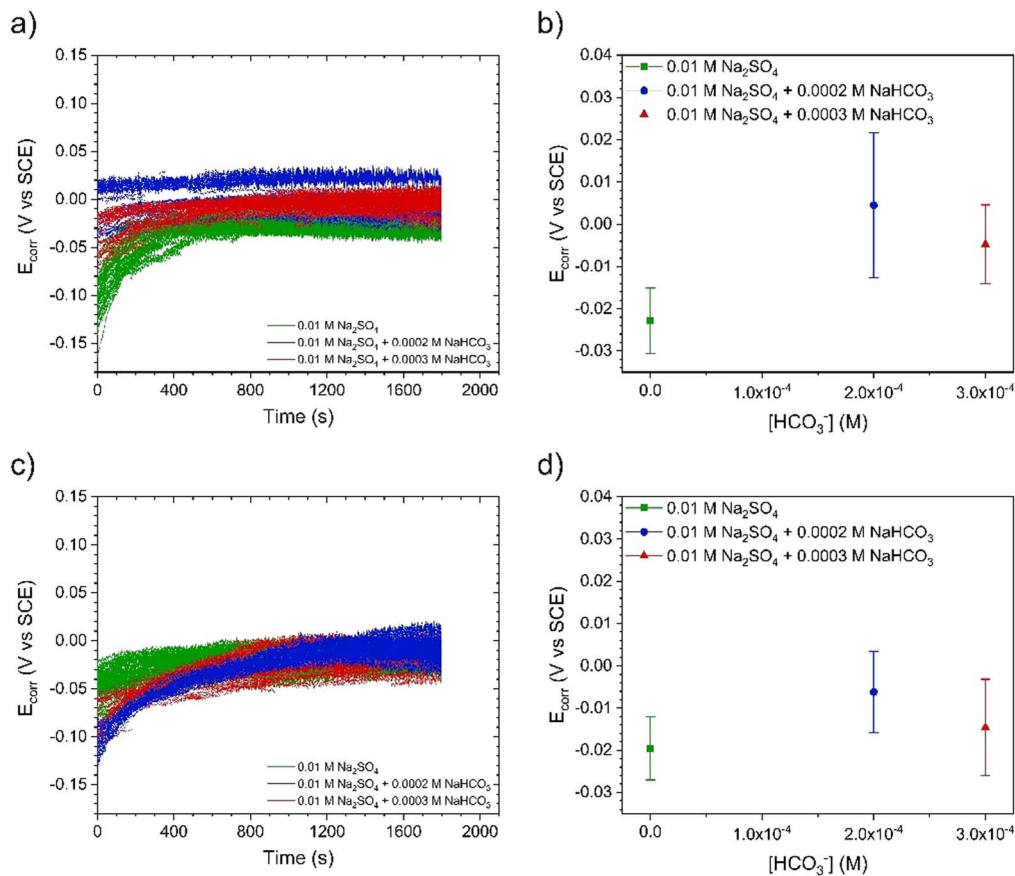


Figure 5. Corrosion potential of Cu electrodes in 0.01 M SO_4^{2-} solution with different $[\text{HCO}_3^-]$; (a), (c) E_{corr} values of Cu in solutions containing 0, 0.2 and 0.3 mM HCO_3^- at pH 8 and pH 9, respectively, (b), (d) comparison of mean and standard deviation of E_{corr} values on Cu electrodes in solutions containing 0, 0.2 and 0.3 mM HCO_3^- at pH 8 and pH 9, respectively.

Statistical Analysis

The group measurements of E_{corr} , E_b , and E_{rp} enabled by the multi-electrode array approach made it possible to perform statistical analyses of these parameters to estimate the pitting probability (likelihood of either $E_{\text{corr}} > E_b$ or $E_{\text{corr}} > E_{\text{rp}}$) and repassivation probability (likelihood that $E_{\text{corr}} < E_{\text{rp}}$) of Cu. The procedure was to determine a distribution function for each measured electrochemical parameter and integrate the area of overlap of the normalized distribution function of E_{corr} with that of either E_b or E_{rp} to yield a pitting or repassivation probability value. Each set of data was fitted with various unknown distribution functions to calculate the predicted pitting or repassivation probability for every combination of distribution function pairs. Kolmogorov–Smirnov test is used to identify proper distributions for E_{corr} , E_b , and E_{rp} to calculate the overlap. A comprehensive statistical treatment process can be found in our previous paper.⁶⁹

Results and Discussion

Effect of sulfate concentration and pH on E_{corr} .—Figure 1 shows the E_{corr} of all electrodes measured in solutions with different $[\text{SO}_4^{2-}]$ and pH. At all concentrations of SO_4^{2-} , E_{corr} increased with time due to the formation of an oxide film on the Cu surface.^{4,71} At pH 8 (Fig. 1a), the average E_{corr} shifted to slightly more negative values as $[\text{SO}_4^{2-}]$ was increased up to 0.01 M, and then dropped significantly with a further increase to 0.1 M. The distribution range of E_{corr} values as expressed by the standard deviation did not change for all concentrations at pH 8 (Fig. 1b). There is a competition between the adsorption of OH^- and SO_4^{2-} on the oxide surface^{9–11}; as a result, SO_4^{2-} interferes with oxide film formation, whilst OH^-

promotes film growth. Al-Khariafi³³ discussed the competition between the adsorption of halide ions and OH^- on the copper surface and reported that halides with a larger ionic radius yields a lower Cu dissolution rate; although, Kong⁵¹ proposed that the ability of halide ions to polarize copper is directly proportional to the size of the ions and a larger peak current density was observed for halides with a larger radius. In our case, E_{corr} decreased with increasing $[\text{SO}_4^{2-}]$, which is in good agreement with our observation in chloride-containing solution,⁶⁹ but it is not in good agreement with the results of Ochoa et al.,⁷² who showed that E_{corr} increased slightly with increasing $[\text{SO}_4^{2-}]$. The reason for this discrepancy could be that Ochoa et al.⁷² did not acquire enough data to properly define the trend; however, in this study, 60 data acquired in two runs of 30 simultaneous measurements were averaged.

When the pH was increased to 9, the distribution in values of E_{corr} decreased in width with increasing $[\text{SO}_4^{2-}]$ (Fig. 1d) compared to the range recorded at pH 8. As a result, there is a critical $[\text{OH}^-]$ above which the distribution range of E_{corr} will decrease with increasing $[\text{SO}_4^{2-}]$. The distribution of E_{corr} values may affect the pitting and repassivation probabilities by changing the overlap between values of E_{corr} , E_b and E_{corr} , E_{rp} respectively.

Effect of sulfate concentration and pH on E_b .—The pitting potentials (E_b) measured in solutions containing different $[\text{SO}_4^{2-}]$ and $[\text{OH}^-]$ are plotted in Fig. 2. At both pH 8 and pH 9, E_b shifted toward negative potentials with increasing $[\text{SO}_4^{2-}]$, indicating a decrease in the protectiveness of the film at higher $[\text{SO}_4^{2-}]$.⁷³ However, increasing the pH shifted E_b to more positive values (Figs. 2b, 2d).^{22,57,58} The relationship between E_b and $\log [\text{SO}_4^{2-}]$ appears to be linear and can be represented by Eq. 1^{72,74,75}:

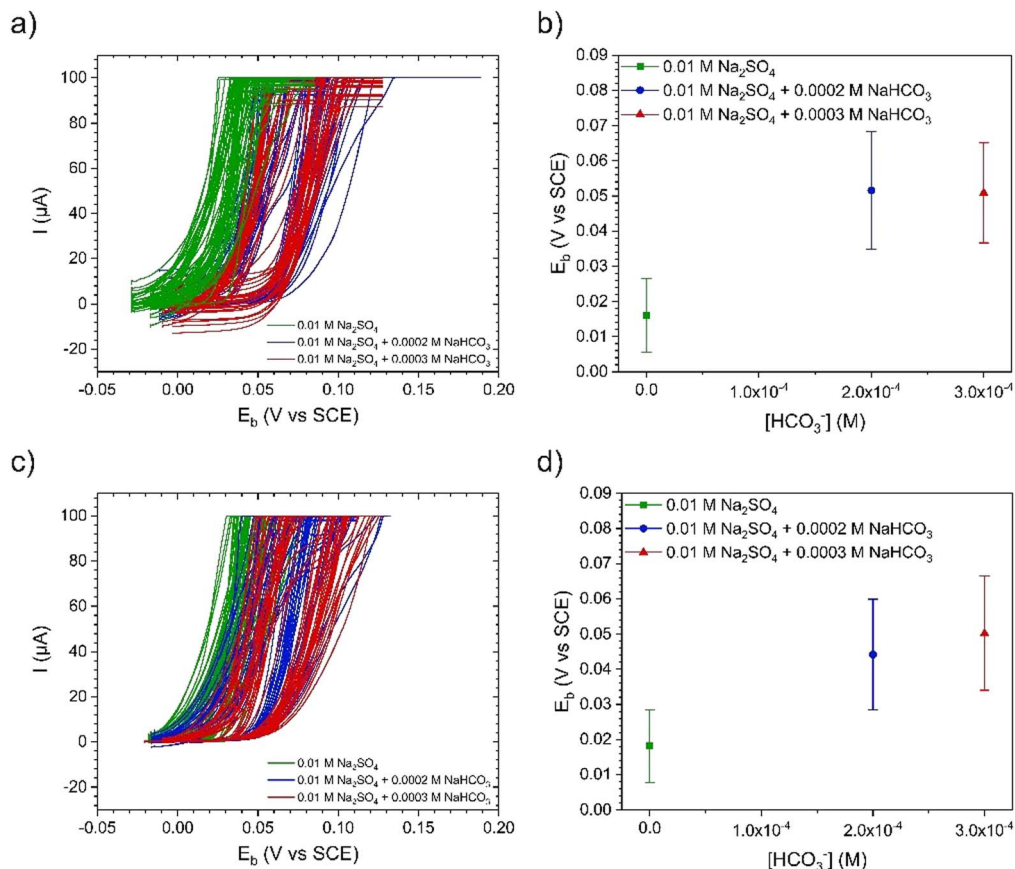


Figure 6. Breakdown potential of Cu electrodes in 0.01 M SO_4^{2-} solution with different $[\text{HCO}_3^-]$: (a), (c) E_b values of Cu in solutions containing 0.2 and 0.3 mM HCO_3^- at pH 8 and pH 9, respectively, (b), (d) comparison of mean and standard deviation of E_b values on Cu electrodes in solutions containing 0.2 and 0.3 mM HCO_3^- at pH 8 and pH 9, respectively.

$$E_b = A - B \log[\text{SO}_4^{2-}] \quad [1]$$

With an increase in the concentration of aggressive anions up to a certain level, the adsorption of aggressive anions such as SO_4^{2-} became more favourable than OH^- adsorption, leading to a shift in E_b to a more negative value. As a result, the distribution of E_b would be more likely to be below the distribution of E_{corr} , resulting in a higher probability of passive film breakdown. Another factor that will influence the pitting probability is the distribution range of E_b . The distribution range of E_b in sulfate-containing solutions at pH 8 did not change significantly with $[\text{SO}_4^{2-}]$, while for pH 9 the distribution range was wide at small concentrations (0.001 M and 0.005 M) but became very narrow at higher concentrations (0.01 M and 0.1 M). These results showed that the pitting probability, as expressed by the distribution range of E_b , was dependent on both $[\text{SO}_4^{2-}]$ and pH.

Based on the distribution curve of corrosion parameters, when the $[\text{SO}_4^{2-}]/[\text{OH}^-]$ ratio is equal to or smaller than 500, then OH^- is the dominant anion enforcing the formation of a dense passive film on the surface. As a result, it would be difficult for $[\text{SO}_4^{2-}]$ to adsorb on the surface and promote passive film breakdown, resulting in a greater distribution range of E_b (Fig. 2d). On the other hand, when $[\text{SO}_4^{2-}]/[\text{OH}^-] > 500$, the distribution range of E_b decreases significantly due to the increased frequency of passive film breakdown. This claim has been made by other researchers,^{50,66,76} but not justified on a statistically relevant scale.

Effect of $[\text{SO}_4^{2-}]$ and pH on E_{rp} .—The E_{rp} of Cu in sulfate-containing solutions at various pH values is shown in Fig. 3.

Increasing $[\text{SO}_4^{2-}]$ shifted E_{rp} to more positive values, the opposite of our observations in chloride-containing solutions.⁶⁹ This increase with increasing $[\text{SO}_4^{2-}]$ may increase the probability to repassivate, depending on and the relative influence on the range of E_{corr} . When the distribution of E_{rp} values is located at potentials lower than the distribution of E_{corr} values, then the area of their overlap indicates the probability that repassivation (as defined by $E_{\text{corr}} < E_{\text{rp}}$) might be possible (Fig. 4). On the other hand, if the distribution of E_{rp} values is located at potentials higher than the distribution of E_{corr} values, the area of overlap indicates the pitting probability (according to our more conservative definition) (Fig. 4).⁵⁵

Many researchers^{37,57,58} have proposed that E_{rp} is not dependent on the concentration of aggressive anions, and our results in good agreement with that proposal. Moreover, our results indicate a dependency of the E_{rp} distribution range on the $[\text{SO}_4^{2-}]$. Increasing the pH shifted the average values of E_{rp} in the negative direction in 0.001 M SO_4^{2-} but exhibited no significant effect at higher $[\text{SO}_4^{2-}]$, as shown in Fig. 3. Our results indicate that $[\text{OH}^-]$ strongly affects the distribution range of E_b values, whereas the distribution ranges of E_{corr} and E_{rp} were not largely affected by $[\text{OH}^-]$.

Effect of bicarbonate on E_{corr} , E_b and E_{rp} .—The E_{corr} values recorded in sulfate-containing solutions with and without HCO_3^- are shown in Fig. 5. At both pH 8 and 9, the addition of HCO_3^- shifted E_{corr} to more positive values and increased the distribution range. The average E_b shifted to more positive values in the presence of HCO_3^- as illustrated in Fig. 6, indicating an increase in the stability of the passive film. The addition of HCO_3^- also increased the distribution range of values, in good agreement with the observation of Li, Frankel and their coworkers^{50,61,66,76–78} regarding the effect of

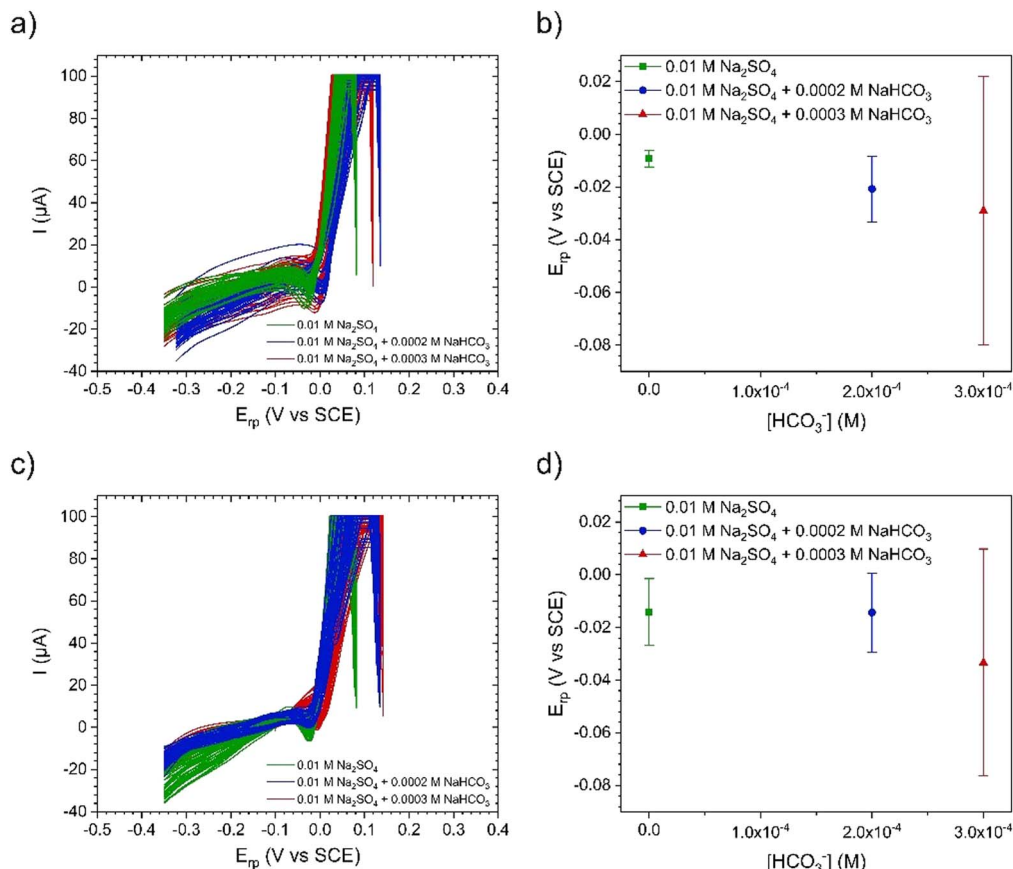


Figure 7. Repassivation potential of Cu electrodes in 0.01 M SO_4^{2-} solution with different $[\text{HCO}_3^-]$; (a), (c) E_{rp} values of Cu in solutions containing 0.2 and 0.3 mM HCO_3^- at pH 8 and pH 9, respectively, (b), (d) comparison of mean and standard deviation of E_{rp} values on Cu electrodes in solutions containing 0.2 and 0.3 mM HCO_3^- at pH 8 and pH 9, respectively.

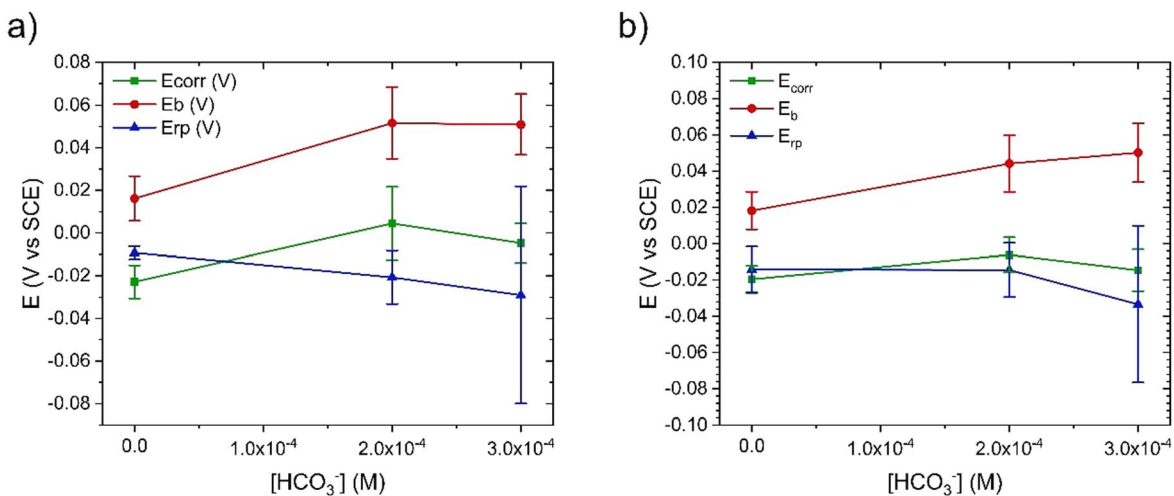


Figure 8. Mean and standard deviation of E_{corr} , E_b , and E_{rp} values of Cu electrodes in 0.01 M SO_4^{2-} solution with different $[\text{HCO}_3^-]$; (a) pH 8 (b) pH 9. The points are the mean and the range represented by the bars is the standard deviation.

passive film quality on the distribution of E_b . The pitting probability of Cu in the presence of HCO_3^- depends on the influence of HCO_3^- on E_b values and their distribution ranges.

Increasing $[\text{HCO}_3^-]$ led to a shift in E_{rp} to more negative values and widened the distribution of values (Fig. 7). Both of these features could increase the probability of repassivation if the distribution curve for E_{rp} was located at potentials lower than the distribution of E_{corr} values. The mean and standard deviations in E_{corr} , E_b , and E_{rp} are plotted in Fig. 8 to demonstrate their relative

positions on the potential scale as a function of $[\text{SO}_4^{2-}]$ and $[\text{HCO}_3^-]$. The probability of film breakdown, as defined by the relative positions of the three key potentials, did not change significantly in the presence of HCO_3^- .

Statistical Analysis

Effect of SO_4^{2-} on pitting and repassivation probabilities.— Histograms and box plot charts of E_{corr} , E_b , and E_{rp} values measured

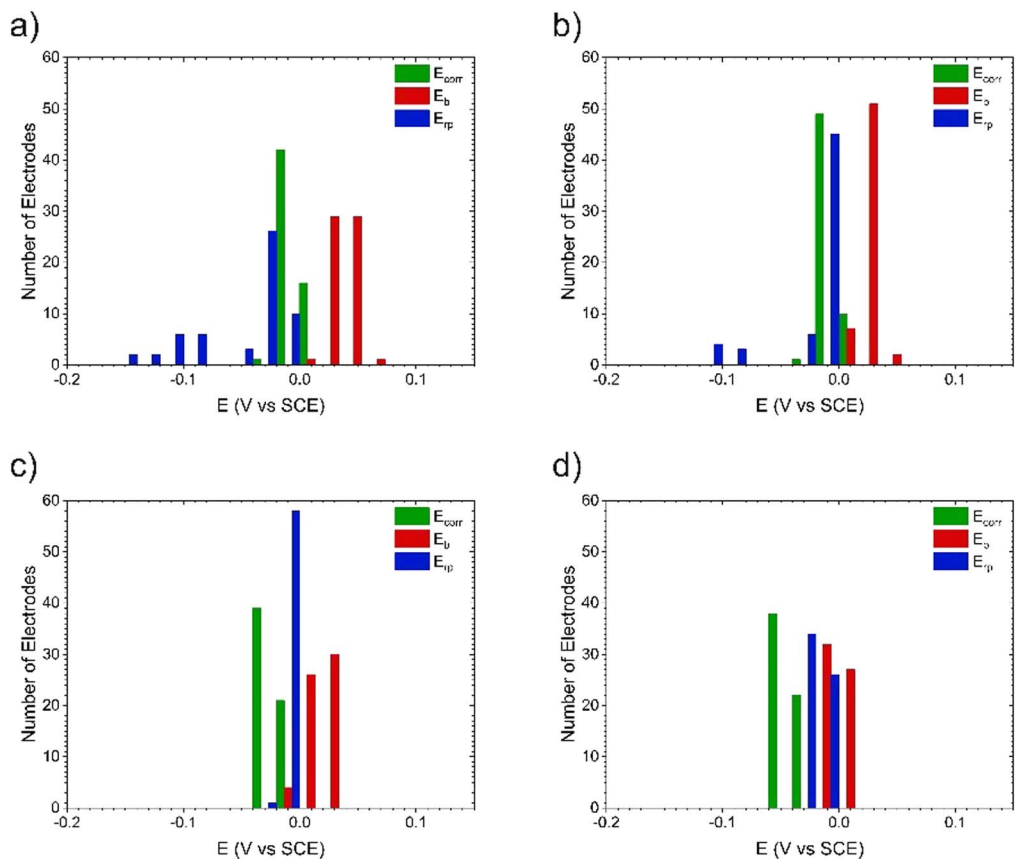


Figure 9. Histograms of E_{corr} , E_b , and E_{tp} values in solutions with various sulfate concentrations at pH 8 (a) 0.001 M (b) 0.005 M (c) 0.01 M (d) 0.1 M.

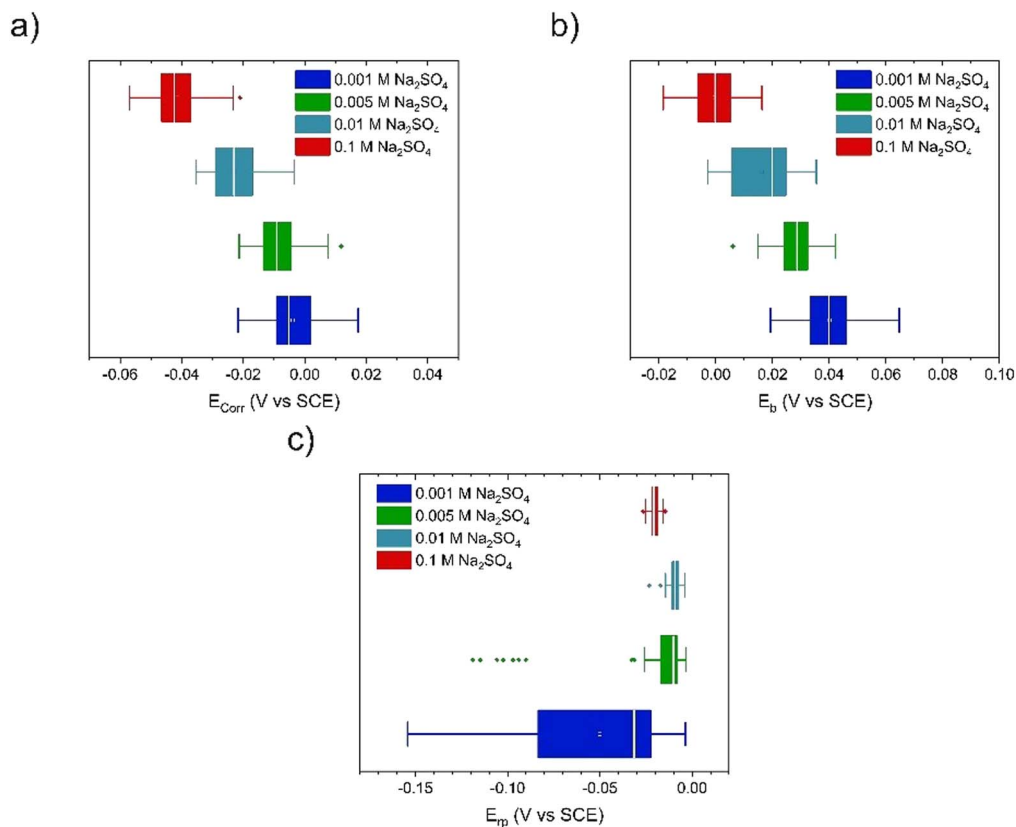


Figure 10. Box plots of corrosion parameters measured on Cu in solutions of different $[\text{SO}_4^{2-}]$ at pH 8 a) E_{corr} , (b) E_b , and (c) E_{tp} .

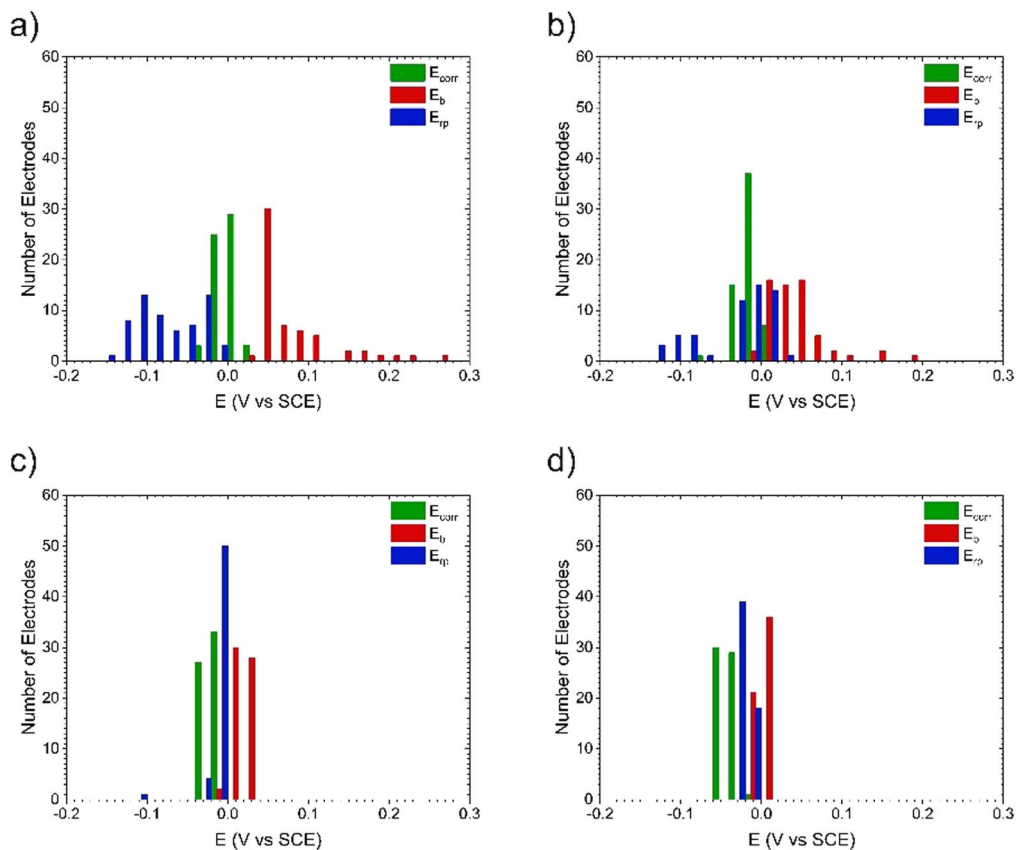


Figure 11. Histograms of E_{corr} , E_b , and E_{rp} values in solutions containing different sulfate concentrations at pH 9 (a) 0.001 M (b) 0.005 M (c) 0.01 M (d) 0.1 M.

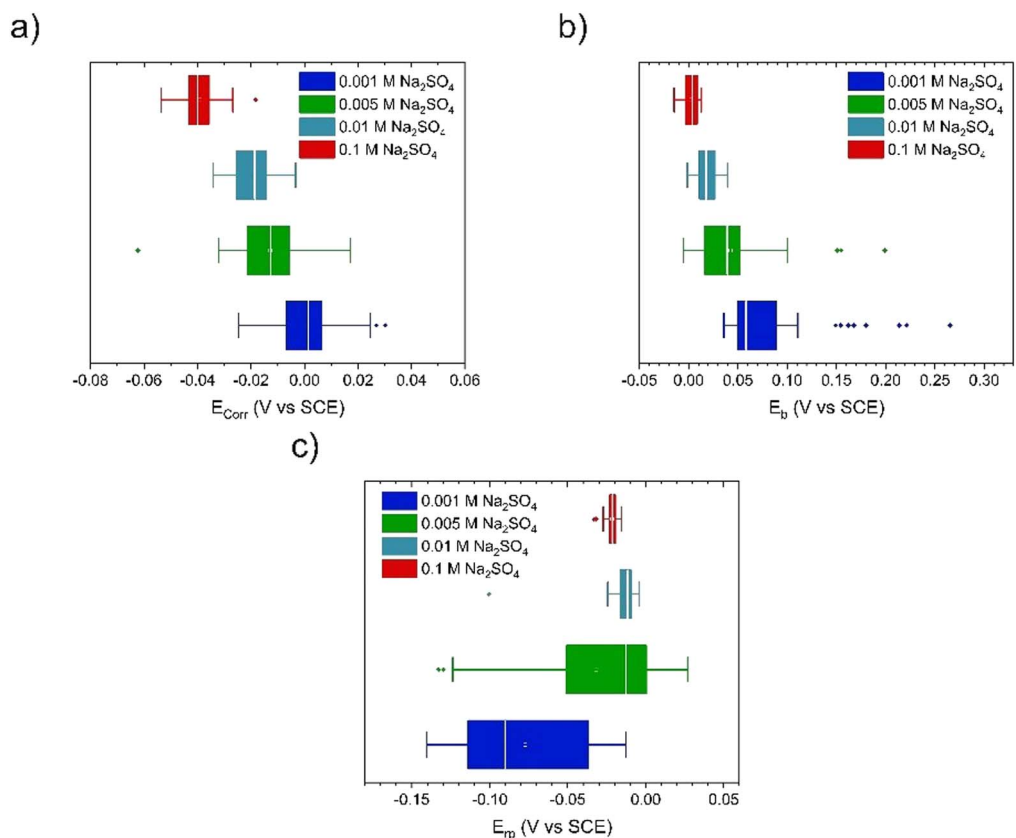


Figure 12. Box plots of corrosion parameters measured on Cu in solutions with different $[SO_4^{2-}]$ at pH 9 a) E_{corr} , (b) E_b , and (c) E_{rp} .

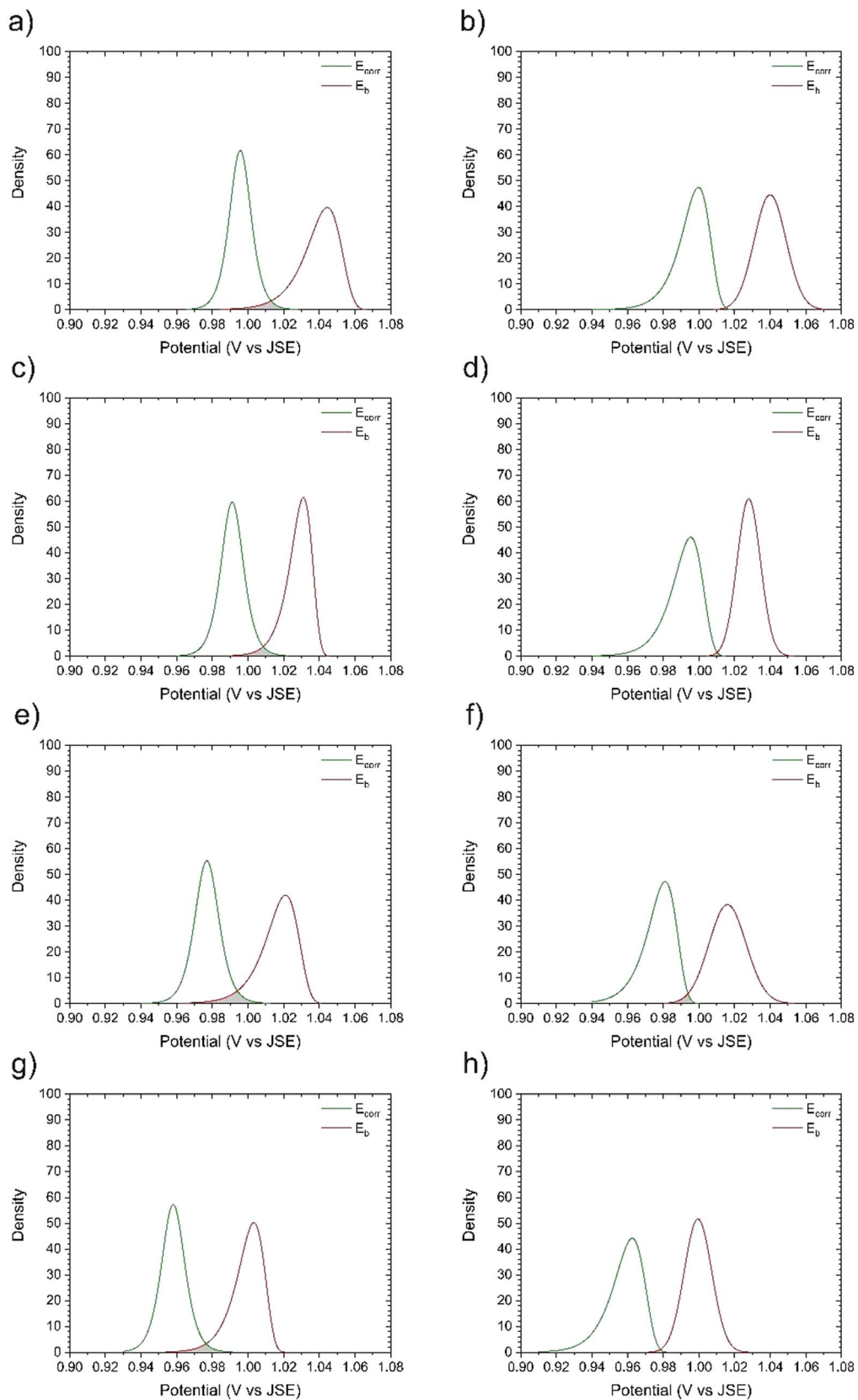


Figure 13. Probability distribution curves of E_{corr} and E_b on Cu in Na_2SO_4 solution of pH 8 at room temperature. Pairs of fitted distribution curves having maximum and minimum overlaps between E_{corr} and E_b , respectively: (a),(b) 0.001 M SO_4^{2-} solution; (c), (d) 0.005 M SO_4^{2-} solution; (e), (f) 0.01 M SO_4^{2-} solution; (g), (h) 0.1 M SO_4^{2-} solution.

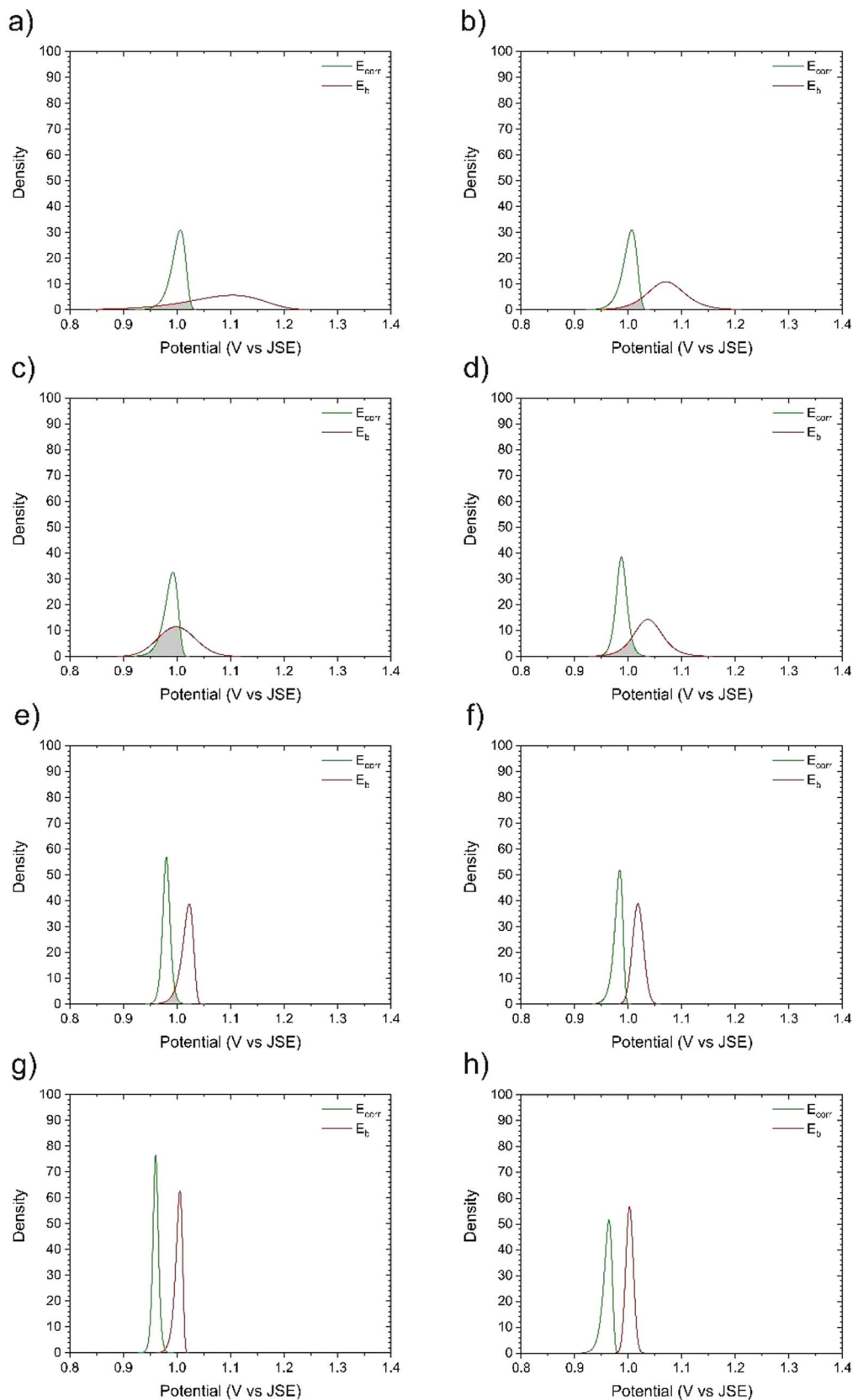


Figure 14. Probability distribution curves of E_{corr} and E_b on Cu in Na_2SO_4 solution of pH 9 at room temperature. Pairs of fitted distribution curves having maximum and minimum overlaps between E_{corr} and E_b , respectively: (a), (b) 0.001 M SO_4^{2-} solution; (c), (d) 0.005 M SO_4^{2-} solution; (e), (f) 0.01 M SO_4^{2-} solution; (g), (h) in 0.1 M SO_4^{2-} solution.

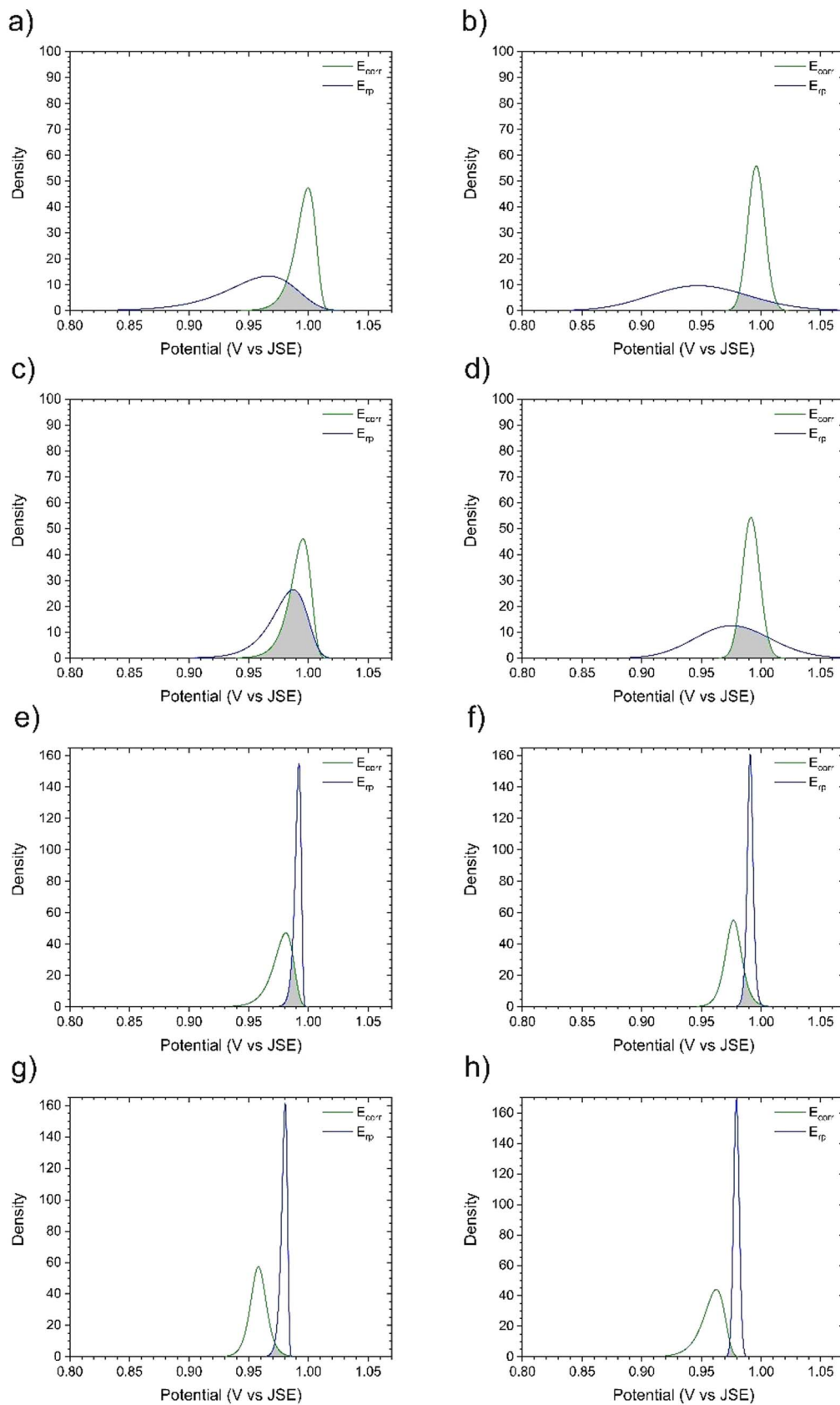


Figure 15. Probability distribution curves for E_{corr} and E_{rp} on Cu in Na_2SO_4 solution of pH 8 at room temperature. Pairs of fitted distribution curves having maximum and minimum overlaps between E_{corr} and E_{rp} , respectively: (a), (b) in 0.001 M SO_4^{2-} solution; (c), (d) 0.005 M SO_4^{2-} solution; (e), (f) 0.01 M SO_4^{2-} solution; (g), (h) 0.1 M SO_4^{2-} solution.

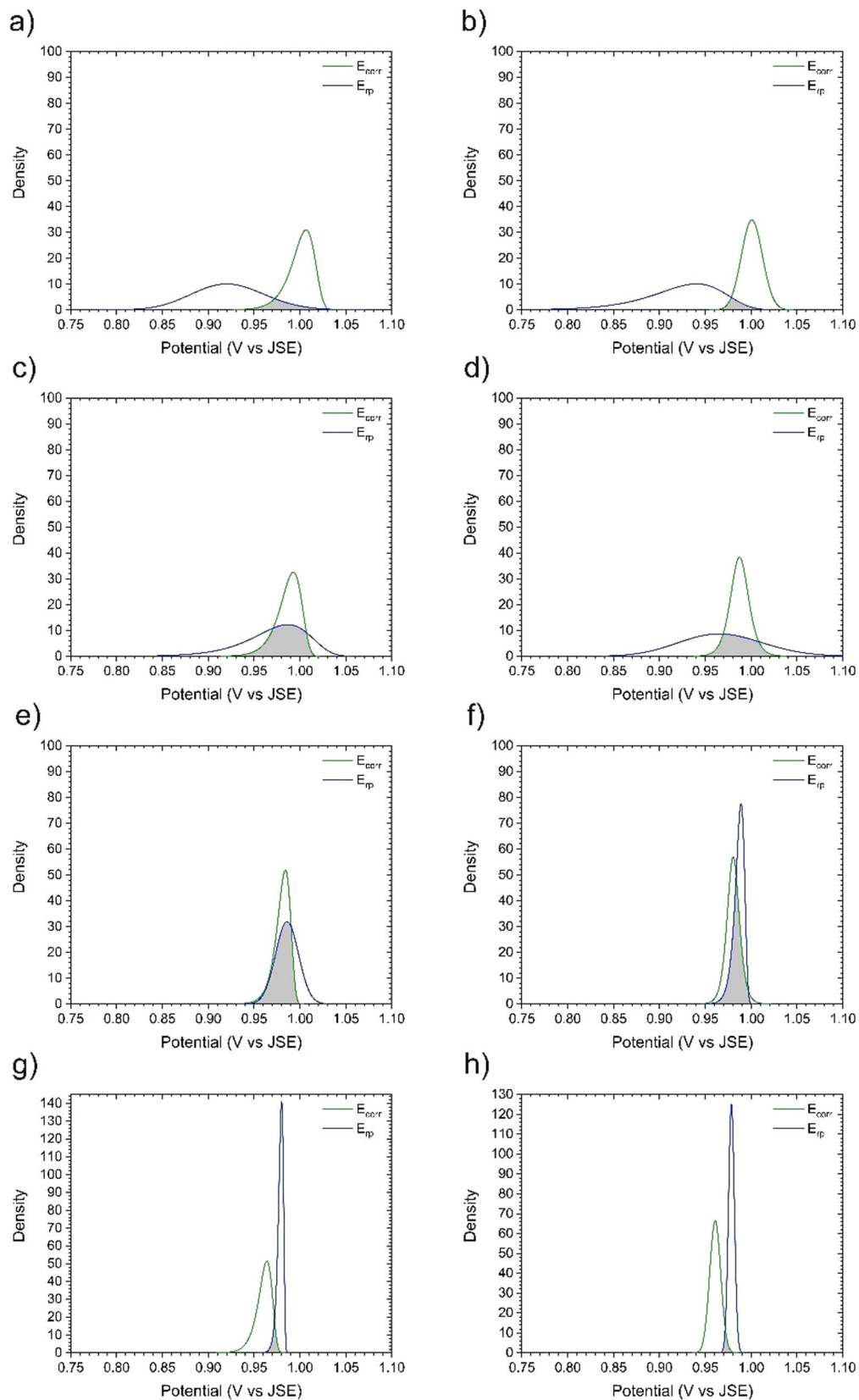


Figure 16. Probability distribution curves for E_{corr} and E_{rp} on Cu in Na_2SO_4 solution of pH 9 at room temperature. Pairs of fitted distribution curves having maximum and minimum overlaps between E_{corr} and E_{rp} , respectively: (a), (b) 0.001 M SO_4^{2-} solution; (c), (d) 0.005 M SO_4^{2-} solution; (e), (f) 0.01 M SO_4^{2-} solution; (g), (h) 0.1 M SO_4^{2-} solution.

Table I. Pitting probability (%) of Cu in sulfate-containing solutions of different concentrations at pH 8: (a) 0.001 M SO₄²⁻; (b) 0.005 M SO₄²⁻; (c) 0.01 M SO₄²⁻; and (d) 0.1 M SO₄²⁻, based on the overlap of different E_b and E_{corr} distribution functions, as indicated.

a) Breakdown potential (E _b)	Distribution	Corrosion potential (E _{corr})				
		Log-logistic	Gamma	Log-Normal	Normal	Weibull
	Log-Logistic	1.57	1.13	1.14	1.12	0.79
	Gamma	1.03	0.62	0.63	0.61	0.33
	Log-Normal	1.01	0.61	0.62	0.60	0.32
	Normal	1.05	0.64	0.65	0.63	0.35
	Weibull	4.55	4.03	4.04	4.01	3.55
b) Breakdown potential (E _b)	Distribution	Corrosion potential (E _{corr})				
		Log-logistic	Gamma	Log-normal	Normal	Weibull
	Log-Logistic	1.67	1.19	1.19	1.17	0.80
	Gamma	1.36	0.88	0.89	0.87	0.51
	Log-Normal	1.36	0.88	0.89	0.86	0.50
	Normal	1.38	0.90	0.90	0.88	0.52
	Weibull	3.81	3.29	3.30	3.27	2.81
c) Breakdown potential (E _b)	Distribution	Corrosion potential (E _{corr})				
		Log-logistic	Gamma	Log-normal	Normal	Weibull
	Log-Logistic	4.87	4.00	4.01	3.97	3.11
	Gamma	3.93	3.05	3.07	3.03	2.17
	Log-Normal	3.91	3.03	3.05	3.01	2.15
	Normal	3.97	3.1	3.11	3.07	2.21
	Weibull	6.58	5.68	5.70	5.65	4.77
d) Breakdown potential (E _b)	Distribution	Corrosion potential (E _{corr})				
		Log-logistic	Gamma	Log-normal	Normal	Weibull
	Log-Logistic	1.82	1.37	1.38	1.36	0.96
	Gamma	1.23	0.80	0.81	0.79	0.01
	Log-Normal	1.22	0.80	0.80	0.78	0.01
	Normal	1.25	0.82	0.83	0.81	0.46
	Weibull	3.92	3.46	3.47	3.44	2.96

in solutions with different [SO₄²⁻] and pH are shown in Fig. 9 through Fig. 12. The histogram and interquartile range (IQR) of E_{corr} for different [SO₄²⁻] at pH 8 indicated the same distribution for all concentrations as illustrated in Figs. 10 and 12. However, outliers were observed on the higher potential side of the IQR for 0.005 M and 0.1 M SO₄²⁻ solutions Fig. 10a, which could suggest an increase in the pitting probability due to the formation of right-skewed distribution curves. In sulfate-containing solutions at pH 9, the IQR became narrower with increasing [SO₄²⁻], resulting in a narrower distribution range as shown in Fig. 12. Outliers were observed on the high-potential side of the distribution curve of E_{corr} in 0.001 M and 0.1 M SO₄²⁻, which could suggest an increase in the pitting probability (i.e., increased overlap between E_{corr} and E_b) (Fig. 12a). On the other hand, outliers were located on the low-potential side of the distribution curve of E_{corr} in 0.005 M SO₄²⁻, which suggests a possible increase in the probability of repassivation (i.e., the overlap between E_{corr} and E_{rp}, with E_{rp} below E_{corr}) (Fig. 12a). The distribution of E_b values did not change significantly with [SO₄²⁻] at pH 8 (Fig. 10b). However, at pH 9, the distribution of E_b values decreased significantly in solutions with [SO₄²⁻] higher than 0.005 M (Fig. 11). Outliers were observed in 0.001 M and 0.005 M SO₄²⁻ at pH 9, which indicates the presence of a significant tail to the distribution curve (left-skewed) that might result in a greater overlap between E_{corr} and E_b values (Fig. 12b). The IQR of E_{rp} decreased with increasing [SO₄²⁻] at both pH 8 and 9, indicating a narrower distribution of values at higher [SO₄²⁻] (Figs. 10c and 12c). Outliers were observed at all [SO₄²⁻] except 0.001 M. These

outliers suggest an increase in the probability of either repassivation or pitting, depending on the position of E_{rp} relative to E_{corr}.

The frequency plots of measured E_{corr}, E_b, and E_{rp} values were fitted with a variety of different distribution functions to determine whether any of these functions provided reasonable representations of the measured data. Some gave reasonable fits whereas others differed significantly from the measured data. In the end, five distribution functions (Normal, Log-normal, Log-logistic, Gamma, and Weibull) were selected for use in the analysis, based on the quality of fit achievable. The probability density functions (PDF) showing the overlap between E_{corr} and E_b in solutions with different [SO₄²⁻] and pH values are shown in Figs. 13 and 14. All combinations of fitted distribution functions were evaluated, but only those that yielded the maximum and minimum degrees of overlap between E_{corr} and E_b at each concentration are plotted in the figures. Note that the application of these statistical analyses required that all of the potential values be positive numbers, to avoid the complications of a sign change in the independent variable within the distribution range; to that end we conceived and used an artificial potential scale, designated “JSE”, representing an arbitrarily chosen potential reference point selected solely to yield positive potential values for all measurements (i.e., a simple translation of all values along the potential axis to make them all have a positive sign).

The maximum pitting probability of Cu estimated in this fashion did not change significantly with increasing [SO₄²⁻] from 1 mM to 0.1 M at pH 8 and was in the range of 3.81% – 6.58% (Table I). The highest pitting probability was observed in 0.01 M SO₄²⁻. An

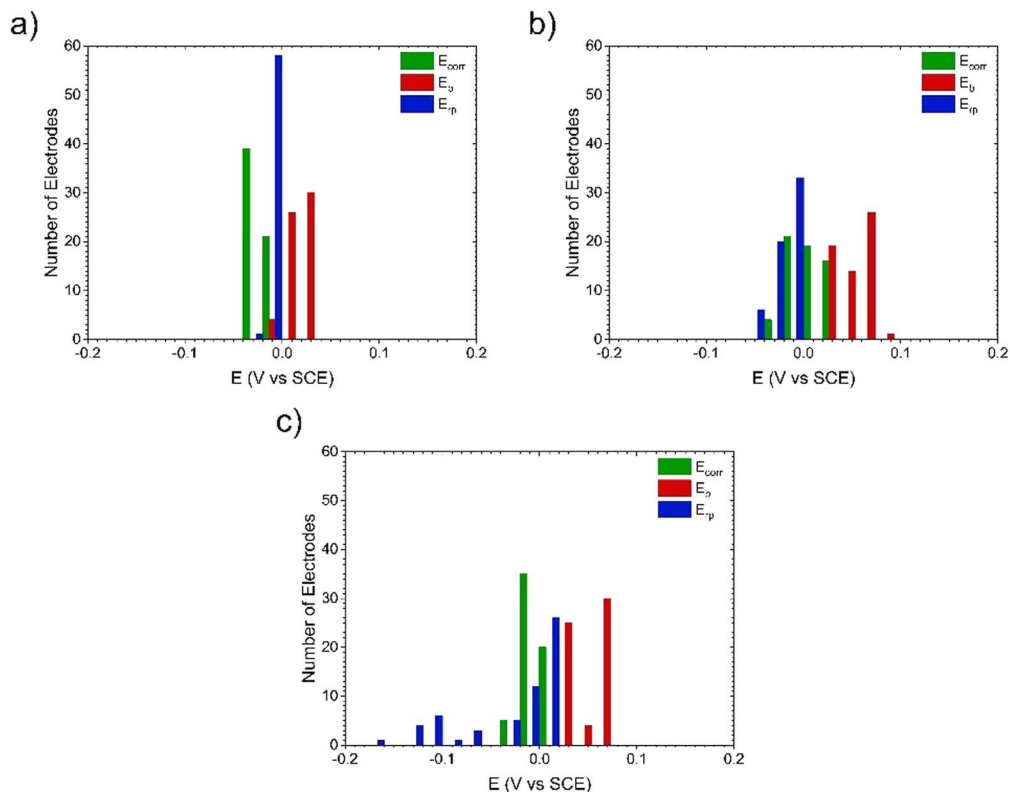


Figure 17. Histogram of E_{corr} , E_b , and E_{rp} values in sulfate-containing solutions with various bicarbonate concentrations at pH 8: (a) 0.01 M SO_4^{2-} ; (b) 0.01 M SO_4^{2-} + 0.0002 M HCO_3^- ; and (c) 0.01 M SO_4^{2-} + 0.0003 M HCO_3^- .

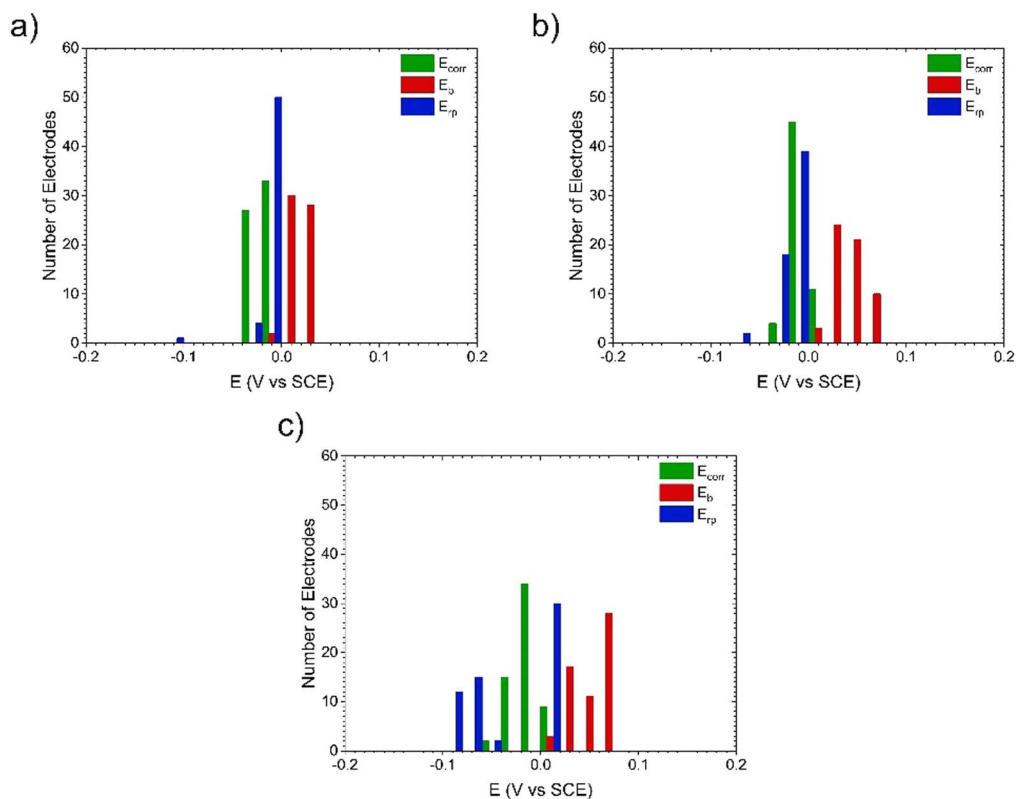


Figure 18. Histogram of E_{corr} , E_b , and E_{rp} values in sulfate-containing solutions with various bicarbonate concentrations at pH 9: (a) 0.01 M SO_4^{2-} ; (b) 0.01 M SO_4^{2-} + 0.0002 M HCO_3^- ; and (c) 0.01 M SO_4^{2-} + 0.0003 M HCO_3^- .

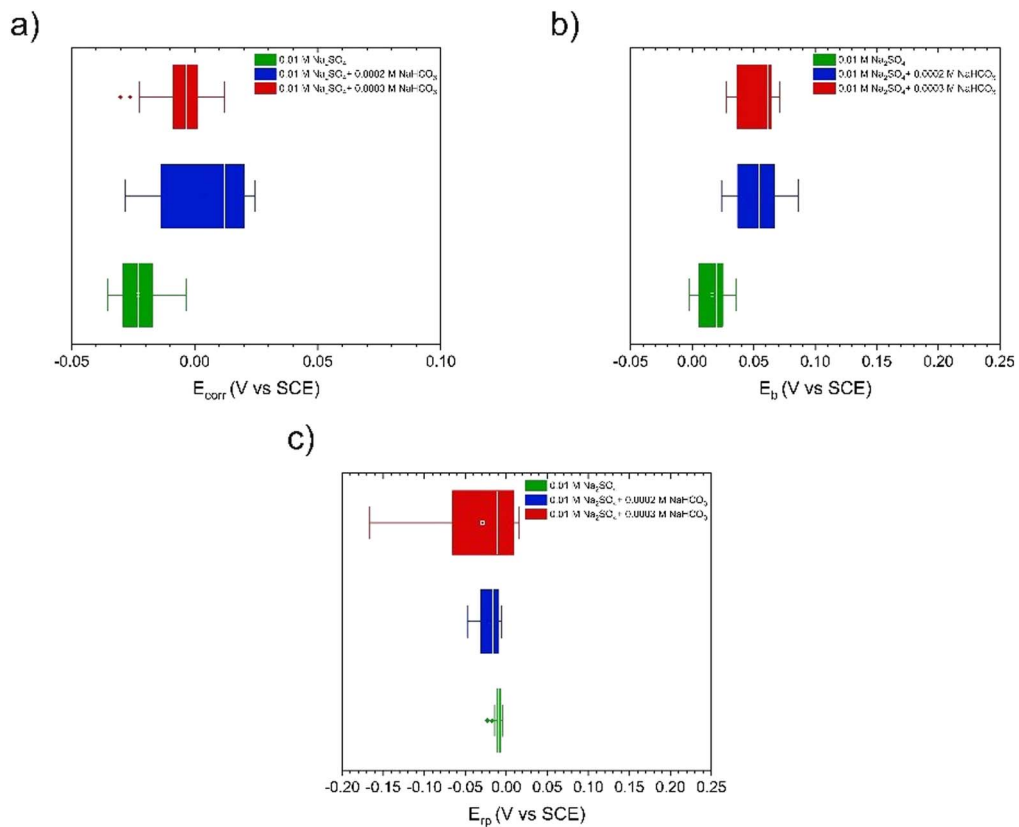


Figure 19. Box plot of corrosion parameters measured on Cu in sulfate-containing solutions with various $[\text{HCO}_3^-]$ at pH 8: (a) E_{corr} ; (b) E_b ; and (c) E_{rp} .

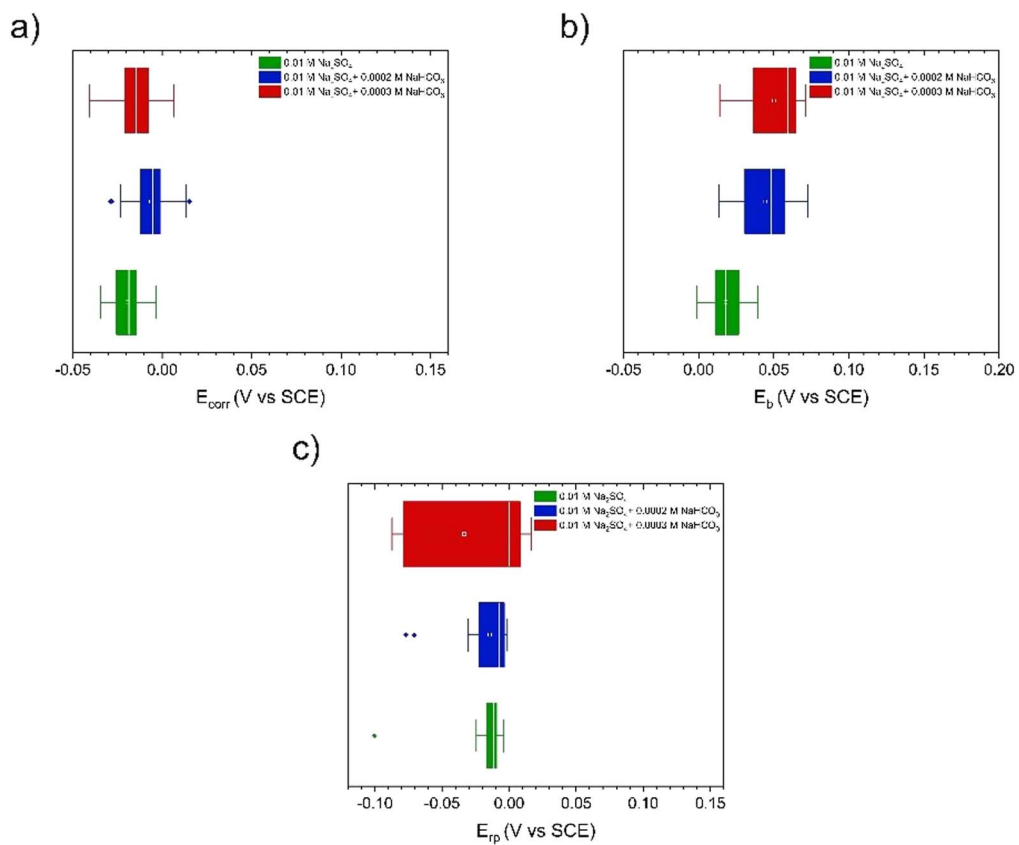


Figure 20. Box plot of corrosion parameters measured on Cu in sulfate-containing solutions with various $[\text{HCO}_3^-]$ at pH 9: (a) E_{corr} ; (b) E_b ; and (c) E_{rp} .

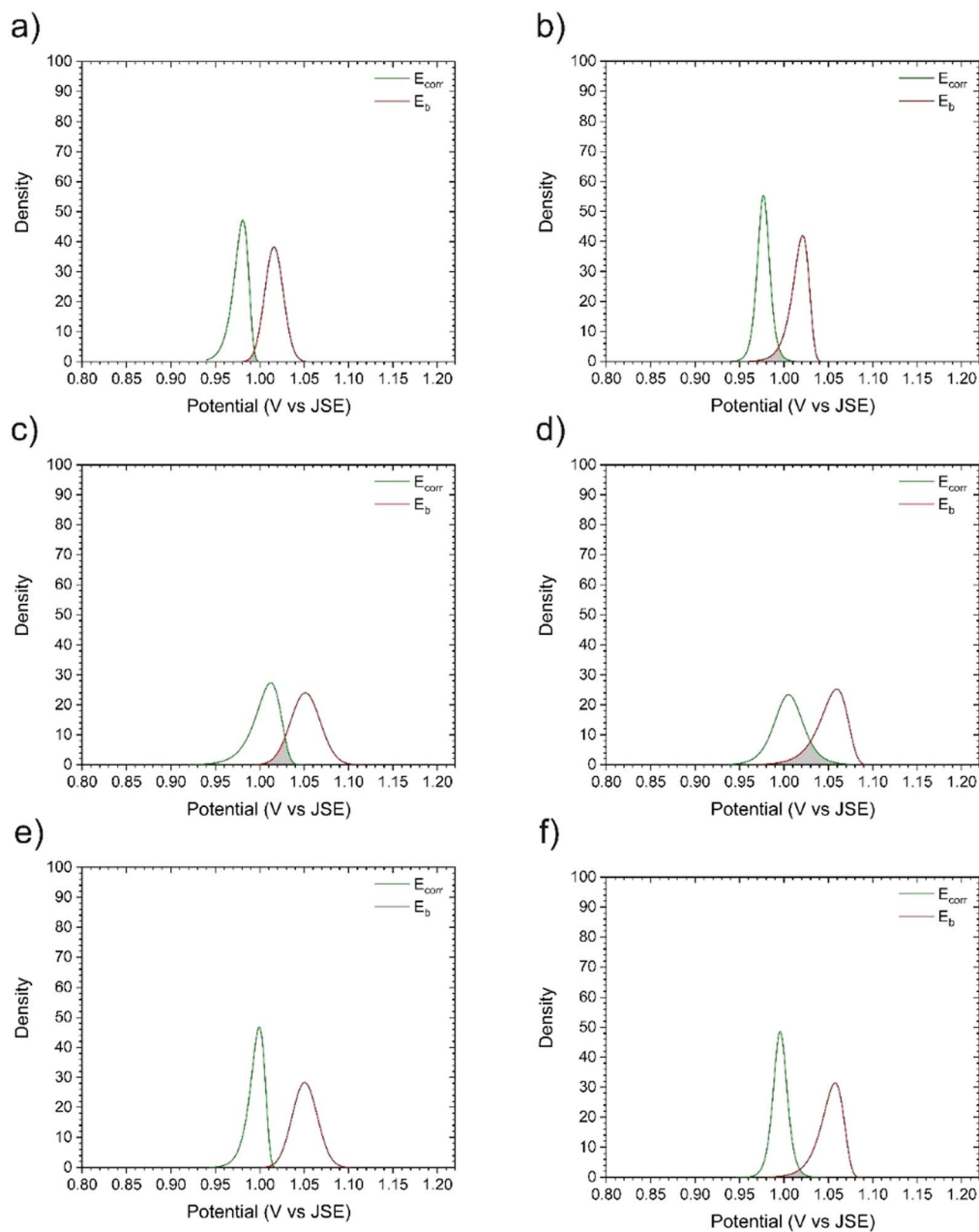


Figure 21. Probability distribution curves for E_{corr} and E_b on Cu in Na_2SO_4 solutions with various $[\text{HCO}_3^-]$ at pH 8 and room temperature. Pairs of fitted distribution curves having minimum and maximum overlaps between E_{corr} and E_b , respectively: (a), (b) 0.01 M SO_4^{2-} solution; (c), (d) 0.01 M SO_4^{2-} + 0.0002 M HCO_3^- solution; (e), (f) 0.01 M SO_4^{2-} + 0.0003 M HCO_3^- solution.

increase in $[\text{SO}_4^{2-}]$ up to 0.01 M led to an increase in pitting probability (Table I), a further increase in $[\text{SO}_4^{2-}]$ to 0.1 M caused the probability of pitting to decrease.

Increasing the pH from 8 to 9 shifted the critical $[\text{SO}_4^{2-}]$ to 0.005 M with the highest pitting probability of 53.26% (Table SI), an approximately one order of magnitude respective decrease in the critical $[\text{SO}_4^{2-}]$ and increase in the pitting probability, demonstrating the strong effects pH has on the pitting process on Cu. A higher pH resulted in a much wider distribution of E_b values, due to the formation of a more protective passive film, which makes it more difficult for aggressive anions to diffuse into the passive film and induce film breakdown.^{48,68} There is a critical concentration (C_{crit}) above which the range of E_b values (Fig. 12b) decreases significantly, contributing to a lower pitting probability of Cu as shown in Table SI. Our results indicate that the reliability of predictions on the corrosion outcome for Cu under these conditions (e.g., whether

pitting corrosion will occur) is dependent on acquisition of a statistically significant^a number of experimental data, due to the stochastic nature of the various corrosion parameters.

The samples were drawn from the same distribution which specified in the null hypothesis if the p-value is greater than the significance level (the specific level is 0.1 in our analysis).

The overlap between the PDFs of E_{corr} and E_{rp} indicates the probability of either repassivation or pitting depending on the position of the E_{rp} distribution relative to that of E_{corr} (Figs. 15 and 16 note that all combinations of fitted distribution functions were evaluated, but only those that yielded the maximum and minimum

^aIn this case, statistically significant implies sufficient to clearly define a distribution function for the parameters in question. The null hypothesis or test statistically significant in K-S test is accepted (the null hypothesis in this paper is that the data comes from a specific distribution) that the samples were drawn from the same distribution which specified in the null hypothesis if the p-value is greater than the significance level (the specific level is 0.1 in our analysis).

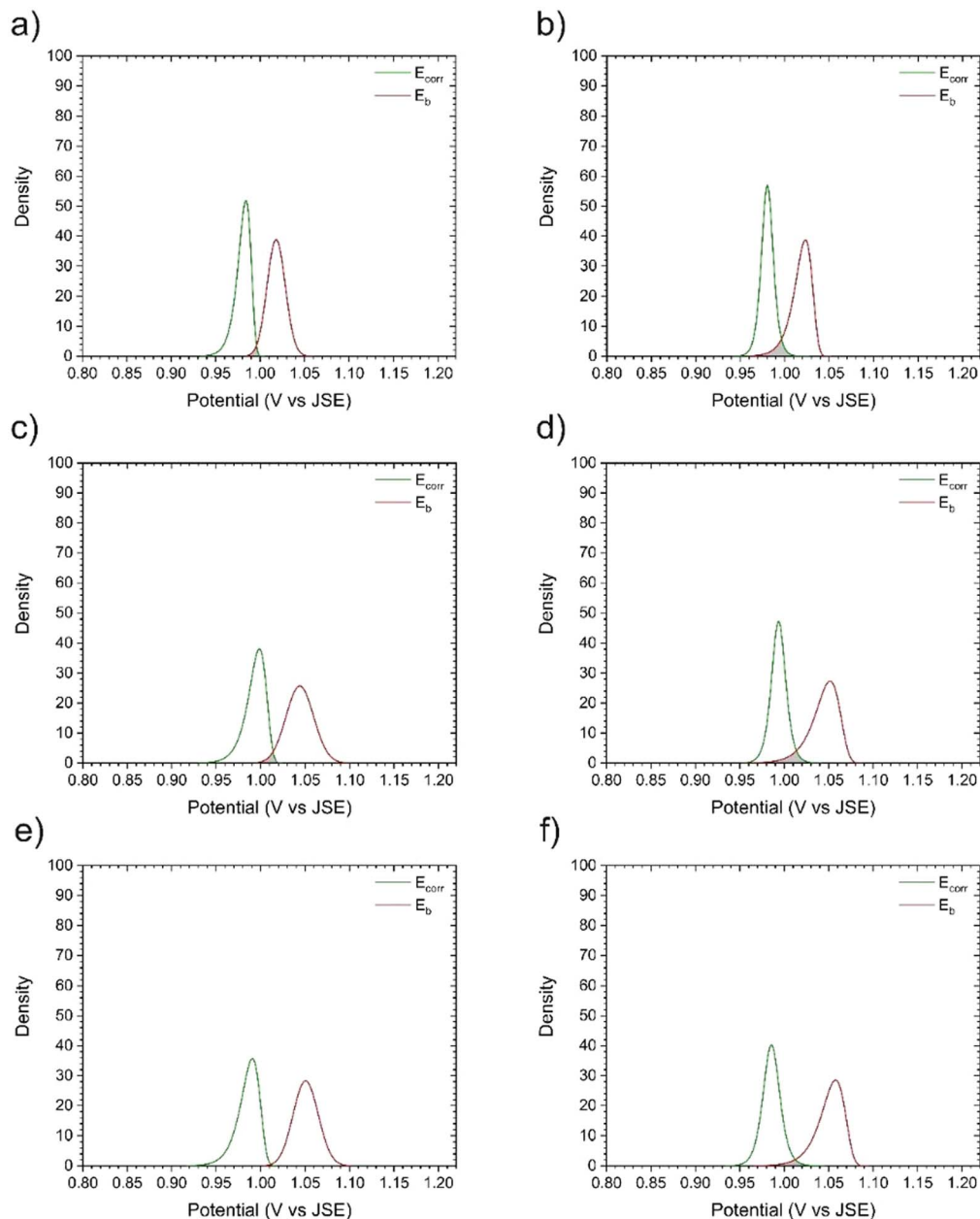


Figure 22. Probability distribution curves for E_{corr} and E_b on Cu in Na_2SO_4 solution with various $[\text{HCO}_3^-]$ at pH 9 and room temperature. Pairs of fitted distribution curves having minimum and maximum overlaps between E_{corr} and E_b , respectively: (a), (b) 0.01 M SO_4^{2-} solution; (c), (d) 0.01 M SO_4^{2-} + 0.0002 M HCO_3^- solution; (e), (f) 0.01 M SO_4^{2-} + 0.0003 M HCO_3^- solution.

degrees of overlap between E_{corr} and E_{rp} at each concentration are plotted in the figures. The repassivation probability increased with increasing $[\text{SO}_4^{2-}]$ up to 0.005 M; however, the distribution of E_{rp} shifted to higher potentials relative to E_{corr} with a further increase in $[\text{SO}_4^{2-}]$ for both pH 8 and 9. As a result, the overlap between E_{rp} and E_{corr} will provide information about the pitting probability. It is important to note that this shift in potential distributions is dependent only on $[\text{SO}_4^{2-}]$ and not on pH. The greatest repassivation probabilities in sulfate-containing solutions at pH 8 and pH 9 (0.005 M) were 66.48% and 57.63%, respectively. Our results indicate that increasing the SO_4^{2-} up to a certain concentration increases the repassivation probability, but moves the E_{rp} distribution to the right side of the E_{corr} distribution, increasing the likelihood of pitting corrosion and decreasing the probability that the system will repassivate. Our statistical analyses proposed that deciding the best and worst corrosion environments for Cu should be

based on a number of experiments sufficient to clearly define the properties of the distribution curve, such as the type of tail, variance, etc, for each distributed parameter in the system.

Figures 17–20 show the histogram and box plot of E_{corr} , E_b , and E_{rp} in 0.01 M $[\text{SO}_4^{2-}]$ solutions with different $[\text{HCO}_3^-]$ and pH. The probability density functions (PDF) for E_{corr} and E_b in 0.01 M $[\text{SO}_4^{2-}]$ solutions with different $[\text{HCO}_3^-]$ and pH, and the overlap between them, are shown in Figs. 21 and 22. The highest overlapping probability increased from 6.58% to 21.20% with the addition of 0.0002 M HCO_3^- at pH 8 and dropped dramatically to around 4.48% when the concentration of HCO_3^- was increased to 0.0003 M (Table SIV). This analysis revealed that adding 0.0002 M $[\text{HCO}_3^-]$ resulted in a wider distribution range of E_{corr} and E_b values (Figs. 23a and 23b), which in turn led to a higher pitting probability. This makes the C_{crit} of anions the key parameter in determining the pitting behaviour. The distribution range of E_{corr} values in a 0.01 M

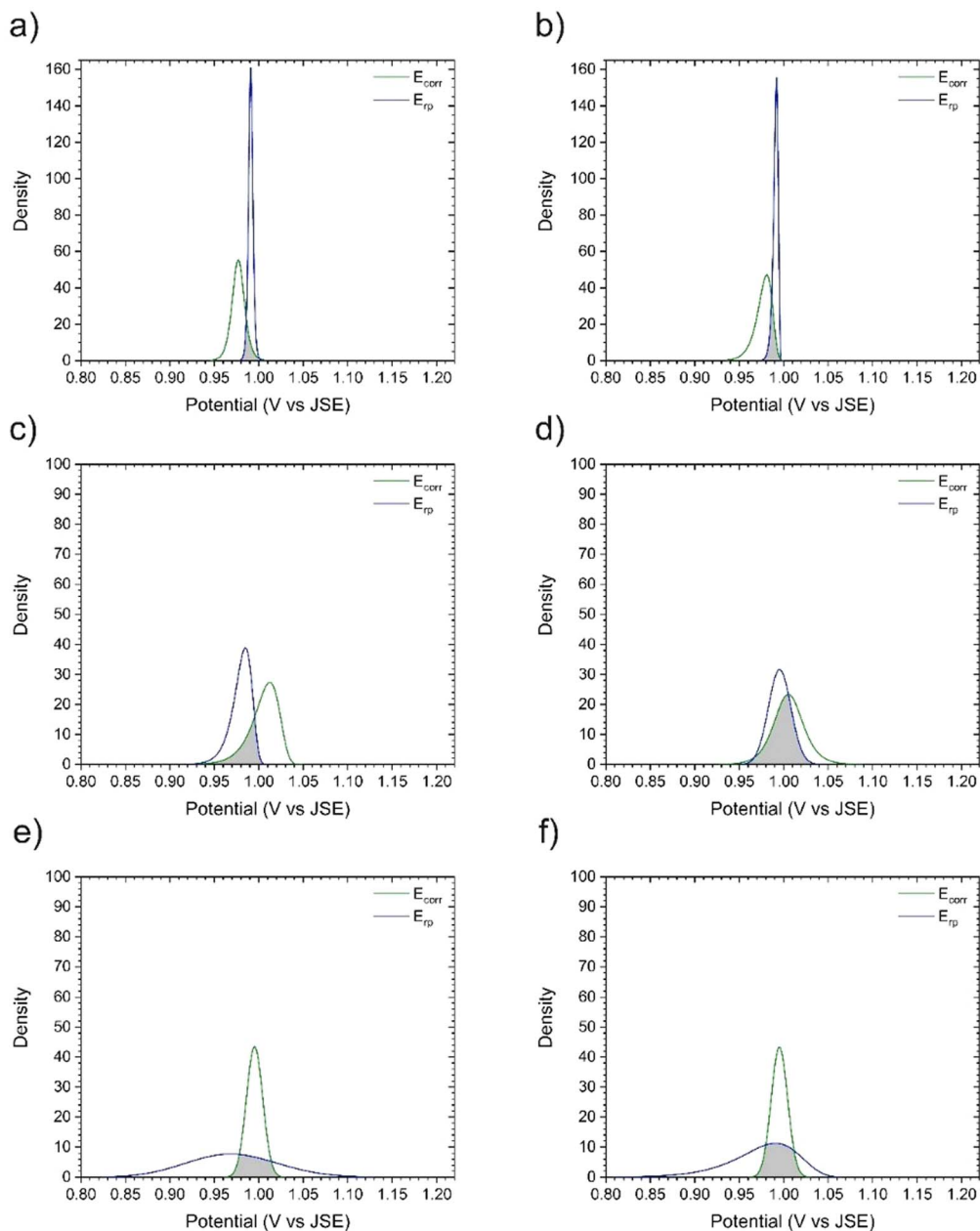


Figure 23. Probability distribution curves for E_{corr} and E_{tp} on Cu in Na_2SO_4 solution with various $[\text{HCO}_3^-]$ at pH 8 and room temperature. Minimum and maximum overlaps between E_{corr} and E_{tp} , respectively: (a), (b) 0.01 M SO_4^{2-} solution; (c), (d) 0.01 M SO_4^{2-} + 0.0002 M HCO_3^- solution; and (e), (f) 0.01 M SO_4^{2-} + 0.0003 M HCO_3^- solution.

SO_4^{2-} solution at pH 9 did not change significantly with the addition of 0.0002 M HCO_3^- . However, the distribution range of E_{corr} values increased with a further increase of HCO_3^- to 0.0003 M. On the other hand, the distribution range of E_{b} values had a small dependency on HCO_3^- . The effect of HCO_3^- on the pitting probability was found to be minimal, with the highest pitting probabilities in a 0.01 M SO_4^{2-} solution containing 0.0002 M and 0.0003 M HCO_3^- being 7.75% and 4.08%, respectively (Table SV).

Figures 23 and 24 show the overlap between the probability density functions (PDF) of E_{corr} and E_{tp} for Cu electrodes in 0.01 M SO_4^{2-} solutions with various $[\text{HCO}_3^-]$ and pH. The presence of HCO_3^- decreased the E_{tp} distribution range below that of E_{corr} . The addition of 0.0002 M HCO_3^- to a 0.01 M SO_4^{2-} solution at pH 8 increased the pitting probability from 22.5% to nearly 100% and decreased the probability of repassivation to 73.99% (Table SVI). A further increase in $[\text{HCO}_3^-]$ decreased the probability of

repassivation to around 42.27%, indicating that the highest repassivation probability was obtained when the $[\text{HCO}_3^-] = 0.0002$ M. The same behaviour was observed at pH 9 (Table SVII), indicating that pH (in this range) plays an insignificant role in the shift of pitting and repassivation probabilities.

Conclusions

Potentiodynamic experiments to determine the distributions of E_{corr} , E_{b} and E_{tp} were performed, and statistical analyses of the values were obtained, to investigate the pitting and repassivation probabilities of Cu in unary (SO_4^{2-}) and binary ($\text{SO}_4^{2-} + \text{HCO}_3^-$) solutions. We determined that E_{corr} values decreased with increasing $[\text{SO}_4^{2-}]$, due to the higher solubility of Cu oxides. The distribution range of E_{corr} decreased with increasing pH and $[\text{SO}_4^{2-}]$, indicating a lower pitting probability. Also, E_{b} shifted to more positive values

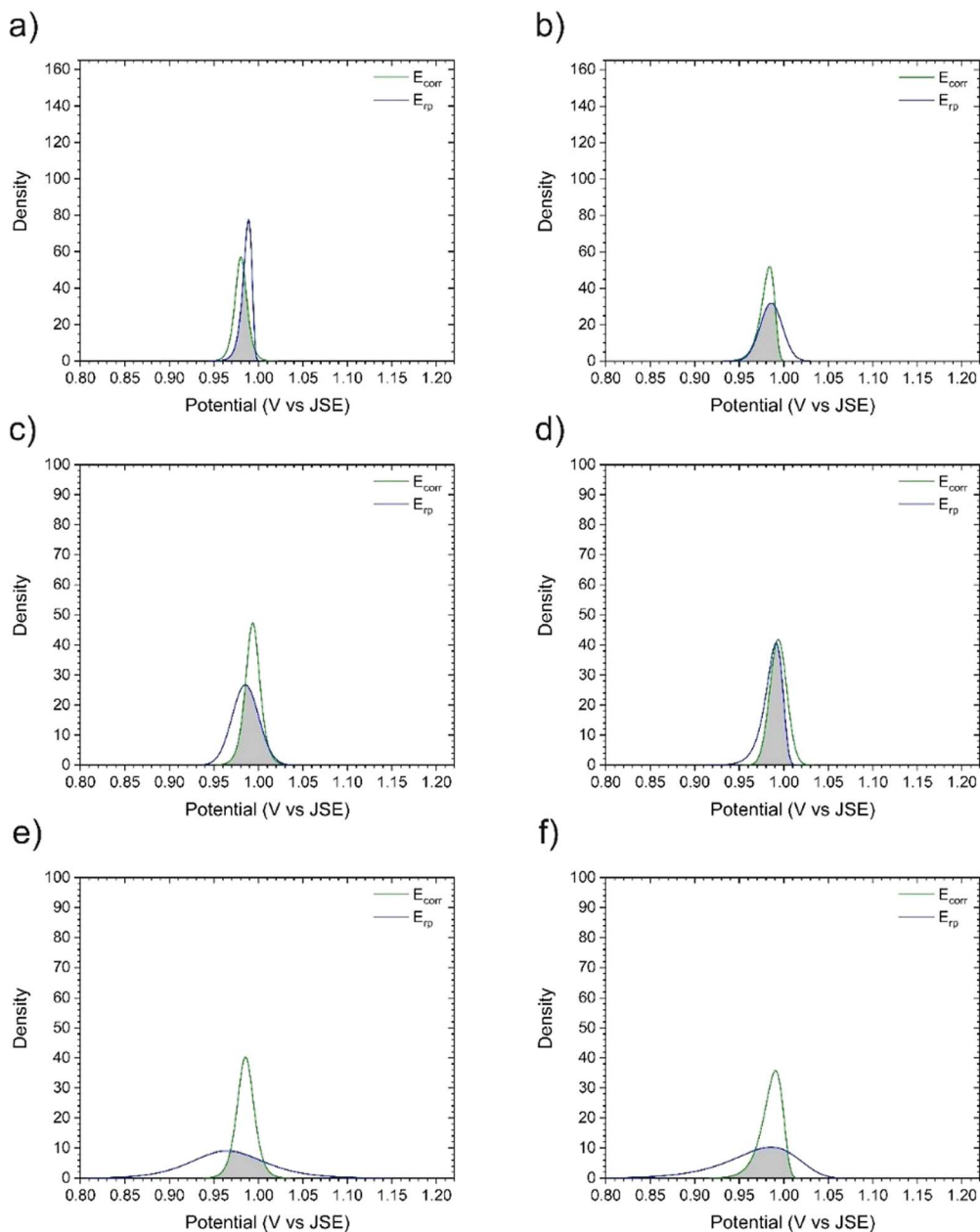


Figure 24. Probability distribution curves for E_{corr} and E_{rp} on Cu in Na_2SO_4 solution with various $[\text{HCO}_3^-]$ of at pH 9 and room temperature. Minimum and maximum overlaps between E_{corr} and E_{rp} , respectively: (a), (b) 0.01 M SO_4^{2-} solution; (c), (d) 0.01 M SO_4^{2-} + 0.0002 M HCO_3^- solution; and (e), (f) 0.01 M SO_4^{2-} + 0.0003 M HCO_3^- solution.

with increasing pH. These observations indicate a relationship between the distribution range of E_b , $[\text{SO}_4^{2-}]$, the pH, and passive film breakdown. Our statistical analyses showed a dependency of E_{rp} on $[\text{SO}_4^{2-}]$. The critical $[\text{SO}_4^{2-}]$ decreased and the pitting probability increased with an increase in pH. The addition of HCO_3^- led to an increase in the resistance to pitting corrosion, as indicated by a shift in E_b to more positive potentials compared to E_b in the same solution without HCO_3^- . The addition of HCO_3^- to a sulfate-containing solution contributed to a negative shift in E_{rp} values.

Acknowledgments

This work was jointly funded by the Natural Sciences and Engineering Research Council of Canada, the Nuclear Waste Management Organization, and the Swedish Nuclear Fuel and Waste Management Company, through Alliance Grant ALLRP561193–20.

Assistance provided by personnel at University Machine Services and Western Nanofabrication Facility is gratefully acknowledged.

ORCID

Sina Matin  <https://orcid.org/0000-0002-5339-9313>

James J. Noël  <https://orcid.org/0000-0003-3467-4778>

References

1. D. S. Hall, M. Behazin, J. W. Binns, and P. G. Keech, "An evaluation of corrosion processes affecting copper-coated nuclear waste containers in a deep geological repository." *Prog. Mater. Sci.*, **118** (2021).
2. "Electric power, annual generation by class of producer." *Statistics Canada, Statistics Canada* (2020).
3. D. S. Hall and P. G. Keech, "An overview of the Canadian corrosion program for the long-term management of nuclear waste." *Corrosion Engineering, Science and Technology*, **52**, 2 (2017).
4. T. Standish, J. Chen, R. Jacklin, P. Jakupi, S. Ramamurthy, D. Zagidulin, P. Keech, and D. Shoemith, "Corrosion of copper-coated steel high level nuclear waste

- containers under permanent disposal conditions." *Electrochim. Acta*, **211**, 331 (2016).
5. C. H. Boyle and S. A. Meguid, "Mechanical performance of integrally bonded copper coatings for the long term disposal of used nuclear fuel." *Nucl. Eng. Des.*, **293**, 403 (2015).
 6. P. G. Keech, P. Vo, S. Ramamurthy, J. Chen, R. Jacklin, and D. W. Shoesmith, "Design and development of copper coatings for long term storage of used nuclear fuel." *Corrosion Engineering, Science and Technology*, **49**, 425 (2014).
 7. J. R. Scully and M. Edwards, "Review of the NWMO copper corrosion allowance." *Nuclear Waste Management Organization* (2013).
 8. G. M. Kwong, "Status of corrosion studies for copper used fuel containers under low salinity conditions." *NWMO, Nuclear Waste Management Organization* (2011).
 9. F. King, C. Lilja, K. Pedersen, P. Pitkänen, and M. Vähänen, "An update of the state-of-the-art report on the corrosion of copper under expected conditions in a deep geologic repository." *SKB* (2010).
 10. F. King, L. Ahonen, C. Taxen, U. Vuorinen, and L. Werme, "Copper corrosion under expected conditions in a deep geologic repository." *SKB* (2002).
 11. F. King, "Corrosion of copper in alkaline chloride environment." *Swedish Nuclear Fuel and Waste Management Co* (2002).
 12. F. King, "Critical review of the literature on the corrosion of copper by water." *Swedish Nuclear Fuel and Waste Management Co* (2010).
 13. G. S. Frankel and N. Sridhar, "Understanding localized corrosion." *Mater. Today*, **11**, 38 (2008).
 14. R. C. Newman, "W.R. Whitney award lecture-understanding the corrosion of stainless steel." *Corrosion*, **57**, 1030 (2001).
 15. N. J. Laycock, M. H. Moayed, and R. C. Newman, "Metastable pitting and the critical pitting temperature." *J. Electrochem. Soc.*, **145**, 2622 (1998).
 16. G. S. Frankel, "Pitting corrosion of metals: a review of the critical factors." *J. Electrochem. Soc.*, **145**, 2186 (1998).
 17. V. M. Salinas-Bravo and R. C. Newman, "An alternative method to determine critical pitting temperature of stainless steels in ferric chloride solution." *Corros. Sci.*, **36**, 66 (1994).
 18. S. T. Pride, J. R. Scully, and J. L. Hudson, "Metastable pitting of aluminum and criteria for the transition to stable pit growth." *J. Electrochem. Soc.*, **141**, 3028 (1994).
 19. P. C. Pistorius and G. T. Burstein, "Metastable pitting corrosion of stainless steel and the transition to stability." *Royal Society London*, **341**, 531 (1992).
 20. G. S. Frankel, L. Stockert, F. Hunkeler, and H. Boehni, "Metastable pitting of stainless steel." *Corrosion*, **43**, 429 (1987).
 21. G. T. Gaudet, W. T. Mo, T. A. Hatton, J. W. Tester, J. Tilly, H. S. Isaacs, and R. C. Newman, "Mass transfer and electrochemical kinetic interactions in localized pitting corrosion, AIChE." *Journal*, **32**, 949 (1986).
 22. J. R. Galvele, "Transport processes and the mechanism of pitting of metals." *J. Electrochem. Soc.*, **123**, 464 (1976).
 23. E. Martinez-Lombardia, Y. Gonzalez-Garcia, L. Lapeire, I. De Graeve, K. Verbeken, L. Kestens, J. M. C. Mol, and H. Terryn, "Scanning electrochemical microscopy to study the effect of crystallographic orientation on the electrochemical activity of pure copper." *Electrochim. Acta*, **116**, 89 (2014).
 24. A. Naser and A. Y. Khan, "A study of growth and breakdown of passive film on copper surface by electrochemical impedance spectroscopy." *Turk. J. Chem.*, **33**, 739 (2009).
 25. K. A. Lill, A. W. Hassel, G. Frommeyer, and M. Stratmann, "Scanning droplet cell investigations on single grains of a FeAlCr light weight ferritic steel." *Electrochim. Acta*, **51**, 978 (2005).
 26. J. Kunze, V. Maurice, L. H. Klein, H.-H. Strehlow, and P. Marcus, "In situ STM study of the duplex passive films formed on Cu(111) and Cu(001) in 0.1 M NaOH." *Corros. Sci.*, **46**, 245 (2004).
 27. C. J. Park, M. M. Lohrengel, T. Hamelmann, M. Pilaski, and H. S. Kwon, "Grain-dependent passivation of surfaces of polycrystalline zinc." *Electrochim. Acta*, **47**, 3395 (2002).
 28. M. Drogowska, L. Brossard, and H. Menard, "Comparative study of copper behaviour in bicarbonate and phosphate aqueous solutions and effect of chloride ions." *J. Appl. Electrochem.*, **24** (1994).
 29. M. R. Gd Chialvo, J. O. Zerbino, and S. L. Marchiano, "Correlation of electrochemical and ellipsometric data in relation to the kinetics and mechanism of Cu₂O electroformation in alkaline solutions." *J. Appl. Electrochem.*, **16**, 517 (1986).
 30. S. B. Adeloju and H. C. Hughes, "The corrosion of copper pipes in high chloride-low carbonate mains water." *Corros. Sci.*, **26**, 851 (1986).
 31. M. R. G. D. Chialvo, R. C. Salvarezza, D. V. Moll, and A. J. Arvia, "Kinetics of passivation and pitting corrosion of polycrystalline copper in borate buffer solutions containing sodium chloride." *Electrochim. Acta*, **30**, 1501 (1985).
 32. M. R. Gd Chialvo and A. J. Arvia, "The electrochemical behaviour of copper in alkaline solutions containing sodium sulphide." *J. Appl. Electrochem.*, **15**, 685 (1985).
 33. F. M. Al-Kharafi and Y. A. El-Tantawy, "Passivation of copper: Role of some anions in the mechanism of film formation and breakdown." *Corros. Sci.*, **22**, 1 (1982).
 34. V. Ashworth and D. Fairhurst, "The anodic formation of Cu₂O in alkaline solutions." *J. Electrochem. Soc.*, **124**, 506 (1977).
 35. D. W. Shoesmith, T. E. Rummery, D. Owen, and W. Lee, "Anodic oxidation of copper in alkaline solutions I. Nucleation and growth of cupric hydroxide films." *J. Electrochem. Soc.*, **123**, 790 (1976).
 36. J. Ambrose, R. G. Barradas, and D. W. Shoesmith, "Investigation of copper in aqueous alkaline solutions by cycling voltammetry." *J. Electroanal. Chem. Interfacial Electrochem.*, **47**, 47 (1973).
 37. I. Milosev, M. Metikos-Hukovic, M. Drogowska, and H. Menard, "Breakdown of passive film on copper in bicarbonate solutions containing sulfate ions." *J. Electrochem. Soc.*, **139**, 2409 (1992).
 38. B. Miller, "Split-Ring disk study of the anodic processes at a copper electrode in alkaline solution." *Journal of Electrochemical Society*, **116** (1969).
 39. H. Cong and J. R. Scully, "Use of coupled multielectrode arrays to elucidate the pH dependence of copper pitting in potable water." *J. Electrochem. Soc.*, **157**, 36 (2010).
 40. H. D. Speckmann, M. M. Lohrengel, J. W. Schultze, and H. H. Strehlow, "The growth and reduction of duplex oxide films on copper." *Ber. Bunsenges. Phys. Chem.*, **89**, 392 (1985).
 41. J. Ambrose, R. G. Barradas, and D. W. Shoesmith, "Rotating copper disk electrode studies of the mechanism of the dissolution-passivation step on copper in alkaline solutions." *J. Electroanal. Chem. Interfacial Electrochem.*, **47**, 65 (1973).
 42. A. Kolics, J. C. Polkinghorne, and A. Wiekowski, "Adsorption of sulfate and chloride ions on aluminum.pdf." *Electrochim. Acta*, **43**, 2605 (1998).
 43. A. G. G. Allah, M. M. Abou-Romia, W. A. Badawy, and H. H. Rehan, "Effect of halide ions on passivation and pitting corrosion of copper in alkaline solutions." *Materials and Corrosion*, **42**, 584 (1991).
 44. N. S. McIntyre, S. Sunder, D. W. Shoesmith, and F. W. Stanchell, "Chemical information from XPS—applications to the analysis of electrode surfaces." *J. Vac. Sci. Technol.*, **18**, 714 (1981).
 45. N. Sato, "A theory for breakdown of anodic oxide films on metals." *Electrochim. Acta*, **16**, 1683 (1971).
 46. X. Wei, C. Dong, P. Yi, A. Xu, Z. Chen, and X. Li, "Electrochemical measurements and atomistic simulations of Cl⁻-induced passivity breakdown on a Cu₂O film." *Corros. Sci.*, **136**, 119 (2018).
 47. S. Y. Yu, W. E. O'Grady, D. E. Ramaker, and P. M. Natishan, "Chloride ingress into aluminum prior to pitting corrosion—an investigation by XANES and XPS." *Journal of Electrochemical Society*, **147** (2000).
 48. H. Cong, H. T. Michels, and J. R. Scully, "Passivity and pit stability behavior of copper as a function of selected water chemistry variables." *J. Electrochem. Soc.*, **156**, 16 (2009).
 49. F. King and C. Lilja, "Localized corrosion of copper canisters." *Corrosion Engineering, Science and Technology*, **49**, 420 (2014).
 50. T. Li, J. Wu, and G. S. Frankel, "Localized corrosion: Passive film breakdown vs Pit growth stability: VI. Pit dissolution kinetics of different alloys and a model for pitting and repassivation potentials." *Corros. Sci.*, **182** (2021).
 51. D. Kong, C. Dong, X. Wei, C. Man, X. Lei, F. Mao, and X. Li, "Size matching effect between anion vacancies and halide ions in passive film breakdown on copper." *Electrochim. Acta*, **292**, 817 (2018).
 52. Z. Qin, R. Daljeet, M. Ai, N. Farhangi, J. J. Noël, S. Ramamurthy, D. Shoesmith, F. King, and P. Keech, "The active/passive conditions for copper corrosion under nuclear waste repository environment." *Corrosion Engineering, Science and Technology*, **52**, 45 (2017).
 53. D. Kong, C. Dong, M. Zhao, X. Ni, C. Man, and X. Li, "Effect of chloride concentration on passive film properties on copper." *Corrosion Engineering, Science and Technology*, **53**, 122 (2017).
 54. H. Ha, C. Taxén, H. Cong, and J. R. Scully, "Effect of applied potential on pit propagation in copper as function of water chemistry." *J. Electrochem. Soc.*, **159**, C59 (2011).
 55. H. Cong and J. R. Scully, "Effect of chlorine concentration on natural pitting of copper as a function of water chemistry." *J. Electrochem. Soc.*, **157**, 200 (2010).
 56. F. King, M. J. Quinn, and C. D. Litke, "Oxygen reduction on copper in neutral NaCl solution." *J. Electrochem. Soc.*, **385**, 45 (1995).
 57. R. M. Souto, S. Gonzalez, R. C. Salvarezza, and A. J. Arvia, "Kinetics of copper passivation and pitting corrosion in Na₂SO₄ containing dilute NaOH aqueous solution." *Electrochim. Acta*, **39**, 2619 (1994).
 58. G. Ruijini, S. C. Srivastava, and M. B. Ives, "Pitting corrosion behavior of UNS N08904 stainless steel in a chloride-sulfate solution." *Corrosion*, **45** (1989).
 59. S. M. Mayanna and T. H. V. Setty, "Role of chloride ions in relation to copper corrosion and inhibition." *Proceedings of the Indian Academy of Sciences - Section A*, **80**, 184 (1974).
 60. H. P. Leckie and H. H. Uhlig, "Environmental factors affecting the critical potential for pitting in 18–8 stainless steel." *J. Electrochem. Soc.*, **113**, 1262 (1966).
 61. T. Li, J. R. Scully, and G. S. Frankel, "Localized corrosion: passive film breakdown vs pit growth stability: part V. Validation of a new framework for pit growth stability using one-dimensional artificial pit electrodes." *J. Electrochem. Soc.*, **166**, C3341 (2019).
 62. S. B. Adeloju and Y. Y. Duan, "Influence of bicarbonate ions on stability of copper oxides and copper pitting corrosion." *Br. Corros. J.*, **29**, 315 (1994).
 63. G. Mankowski, J. P. Duthil, and A. Giusti, "The pit morphology on copper in chloride- and sulphate-containing solutions." *Corros. Sci.*, **39**, 27 (1997).
 64. N. G. Smart and J. O. M. Bockris, "Effect of water activity on corrosion." *Corrosion*, **48**, 277 (1992).
 65. K. Venu, K. Balakrishnan, and K. S. Rajagopalan, "A potentiokinetic polarization study of the behaviour of steel in NaOH-NaCl system." *Corros. Sci.*, **5**, 59 (1965).
 66. G. S. Frankel, T. Li, and J. R. Scully, "Localized corrosion: Passive film breakdown vs pit growth stability." *J. Electrochem. Soc.*, **164**, C180 (2017).
 67. R. Huang, D. J. Horton, F. Bocher, and J. R. Scully, "Localized corrosion resistance of Fe-Cr-Mo-W-B-C bulk metallic glasses containing Mn+Si or Y in neutral and acidified chloride solution." *Corrosion*, **66** (2010).
 68. H. Ha, C. Taxen, K. Williams, and J. Scully, "Effects of selected water chemistry variables on copper pitting propagation in potable water." *Electrochim. Acta*, **56**, 6165 (2011).

69. S. Matin, A. Tahmasebi, M. Momeni, M. Behazin, M. Davison, D. W. Shoesmith, and J. J. Noël, "Use of Multielectrode Arrays and Statistical Analysis to Investigate the Pitting Probability of Copper: I. The Effect of Chloride." *J. Electrochem. Soc.*, **169** (2022).
70. F. Mao, C. Dong, S. Sharifi-Asl, P. Lu, and D. D. Macdonald, "Passivity breakdown on copper: Influence of chloride ion." *Electrochim. Acta*, **144**, 391 (2014).
71. M. A. Abdulhay and A. A. Al-Suhybani, "Open circuit potential for copper electrode in 1 M NaCl solutions." *Materials Science and Engineering Technology*, **23**, 407 (1992).
72. M. Ochoa, M. A. Rodríguez, and S. B. Farina, "Corrosion of high purity copper in solutions containing NaCl, Na₂SO₄ and NaHCO₃ at different temperatures, Procedia." *Mater. Sci.*, **9**, 460 (2015).
73. A. E. Warraky, H. A. E. Shayeb, and E. M. Sherif, "Pitting corrosion of copper in chloride solutions." *Anti-Corrosion Methods and Materials*, **51**, 25 (2004).
74. A. Nishikata, M. Itagaki, T. Tsuru, and S. Haruyama, "Passivation and its stability on copper in alkaline solutions containing carbonate and chloride ions." *Corros. Sci.*, **31**, 287 (1990).
75. G. Bianchi, G. Fiori, P. Longhi, and F. Mazza, "Horse shoe- corrosion of copper alloys in flowing sea water- mechanism, and possibility of cathodic protection of condenser tubes in power generation." *Corrosion*, **34**, 396 (1978).
76. T. Li, J. R. Scully, and G. S. Frankel, "Localized corrosion: passive film breakdown vs pit growth stability: II. A model for critical pitting temperature." *J. Electrochem. Soc.*, **165**, C484 (2018).
77. T. Li, J. R. Scully, and G. S. Frankel, "Localized corrosion: passive film breakdown vs pit growth stability: IV. The role of salt film in pit growth: a mathematical framework." *J. Electrochem. Soc.*, **166**, C115 (2019).
78. T. Li, J. R. Scully, and G. S. Frankel, "Localized corrosion: passive film breakdown vs pit growth stability: III. a unifying set of principal parameters and criteria for pit stabilization and salt film formation." *J. Electrochem. Soc.*, **165**, C762 (2018).